

**THE METALLICITY OF HIGH REDSHIFT GALAXIES:
THE ABUNDANCE OF ZINC IN 34 DAMPED LYMAN α SYSTEMS FROM
 $z = 0.7$ TO 3.4**

MAX PETTINI

Royal Greenwich Observatory, Madingley Road, Cambridge, CB3 0EZ, UK

e-mail: pettini@ast.cam.ac.uk

LINDA J. SMITH

Department of Physics and Astronomy, University College London,

Gower Street, London WC1E 6BT, UK

e-mail: ljs@star.ucl.ac.uk

DAVID L. KING

Royal Greenwich Observatory, Madingley Road, Cambridge, CB3 0EZ, UK

e-mail: king@ast.cam.ac.uk

RICHARD W. HUNSTEAD

School of Physics, University of Sydney, NSW 2006, Australia

e-mail: rwh@physics.usyd.edu.au

ABSTRACT

We report new observations of Zn II and Cr II absorption lines in 10 damped Lyman α systems (DLAs), mostly at redshift $z_{\text{abs}} \gtrsim 2.5$. By combining these results with those from our earlier survey (Pettini et al. 1994) and other recent data, we construct a sample of 34 measurements (or upper limits) of the Zn abundance relative to hydrogen [Zn/H]; the sample includes more than one third of the total number of DLAs known.

The plot of the abundance of Zn as a function of redshift reinforces the two main findings of our previous study. (1) Damped Lyman α systems are mostly metal-poor, *at all redshifts sampled*; the column density weighted mean for the whole data set is [Zn/H] = -1.13 ± 0.38 (on a logarithmic scale), or approximately 1/13 of solar. (2) There is a large spread, by up to two orders of magnitude, in the metallicities we measure at essentially the same redshifts. We propose that damped Lyman α systems are drawn from a varied population of galaxies of different morphological types and at different stages of chemical evolution, supporting the idea of a protracted epoch of galaxy formation.

At redshifts $z \gtrsim 2$ the typical metallicity of the damped Lyman α systems is in agreement with expectations based on the consumption of H I gas implied by the recent measurements of Ω_{DLA} by Storrie-Lombardi et al. (1996a), and with the metal ejection rates in the universe at these epochs deduced by Madau (1996) from the ultraviolet luminosities of high redshift galaxies revealed by deep imaging surveys. There are indications in our data for an increase in the mean metallicity of the damped Lyman α systems from $z > 3$ to ≈ 2 , consistent with the rise in the comoving star formation rate indicated by the relative numbers of *U* and *B* drop-outs in the *Hubble Deep Field*. Although such comparisons are still tentative, it appears that these different avenues

for exploring the early evolution of galaxies give a broadly consistent picture.

At redshifts $z < 1.5$ DLAs evidently do not exhibit the higher abundances expected from a simple closed-box model of global chemical evolution, although the number of measurements is still very small. We speculate that this may be due to an increasing contribution of low surface brightness galaxies to the cross-section for damped Lyman α absorption and to the increasing dust bias with decreasing redshift proposed by Fall and collaborators. However, more DLAs at intermediate redshifts need to be identified before the importance of these effects can be assessed quantitatively.

The present sample is sufficiently large for a first attempt at constructing the metallicity distribution of damped Lyman α systems and comparing it with those of different stellar populations of the Milky Way. The DLA abundance histogram is both broader and peaks at lower metallicities than those of either thin or thick disk stars. At the time when our Galaxy's metal enrichment was at levels typical of DLAs, its kinematics were closer to those of the halo and bulge than a rotationally supported disk. This finding is at odds with the proposal that most DLAs are large disks with rotation velocities in excess of 200 km s^{-1} , based on the asymmetric profiles of absorption lines recorded at high spectral resolution. Observations of the familiar optical emission lines from H II regions, which are within reach of near-infrared spectrographs on 8-10 m telescopes, may help resolve this discrepancy.

Subject headings: cosmology: observations — galaxies: abundances — galaxies: evolution — quasars: absorption lines

1. INTRODUCTION

In the last twelve months there has been a dramatic increase in our ability to identify normal galaxies at $z \simeq 3$, study their stellar populations, and measure the rates of star formation and metal production in the universe over most of the Hubble time (Steidel et al. 1996; Madau et al. 1996). The most prominent features in the spectra of field galaxies at high-redshift (as is the case in the ultraviolet spectra of nearby star-forming galaxies) are strong interstellar lines which are similar, both qualitatively (in the range of ionization stages seen) and quantitatively (in the strengths of the absorption), to those in damped Lyman α systems; this similarity is consistent with the view that this class of QSO absorbers traces the material available for star formation at $z \gtrsim 2$ (e.g. Wolfe 1995). The connection between normal galaxies and damped Lyman α systems (DLAs) is a particularly important one to make and clarifying several aspects of this connection remains a priority. The reason is simple: QSOs with known DLAs are typically more than 5 magnitudes brighter than a L^* galaxy at the same redshift. Consequently, we will inevitably continue to rely mostly on QSO absorption line spectroscopy for the study of physical conditions in the early stages of galaxy formation.

Since 1990 (Pettini, Boksenberg, & Hunstead 1990) we have been conducting a survey of metallicity and dust in DLAs taking advantage of the diagnostic value of weak transitions of Zn II and Cr II. As explained in that paper (see also the critical reappraisal of the technique in Pettini et al. 1997), $[\text{Zn}/\text{H}]^1$ is a straightforward measure of the degree of metal enrichment analogous to the stellar $[\text{Fe}/\text{H}]$, while $[\text{Cr}/\text{Zn}]$ reflects the extent to which grain constituents are removed from the gas phase and thereby gives an indication of the dust-to-metals ratio. The major results of the survey were reported in Pettini et al. (1994). From the analysis of Zn and Cr abundances in 17 DLAs, mostly at $z \simeq 2$, we concluded that the typical metallicity of the universe at a look-back time of ~ 13 Gyr ($H_0 = 50 \text{ km s}^{-1} \text{ Mpc}^{-1}$; $q_0 = 0.01$) was $Z_{\text{DLA}} = 1/10Z_{\odot}$. We further found

¹We use the conventional notation where $[\text{X}/\text{Y}] = \log (\text{X}/\text{Y}) - \log (\text{X}/\text{Y})_{\odot}$

that there is a considerable range—by up to two orders of magnitude—in the degree of metal enrichment reached by different damped Lyman α galaxies at essentially the same epoch, and that even at these early stages of galaxy formation dust appears to be an important component of the interstellar medium, leading to the selective depletion of refractory elements from the gas.

A natural next step is to extend the Zn and Cr abundance measurements over a wider range of redshifts than that considered by Pettini et al. (1994) with the ultimate aim of identifying the emergence of heavy elements and dust in galaxies and following their build-up with time. To this end we have continued our survey since 1994; the full sample now consists of 34 DLAs, more than one third of the total number known (Wolfe et al. 1995). In this paper we present the new data and consider the conclusions that can be drawn from the whole set of measurements of $[\text{Zn}/\text{H}]$; preliminary reports have appeared in conference proceedings (e.g. Pettini et al. 1995a; Smith et al. 1996). Our findings on the abundance of dust from consideration of the $[\text{Cr}/\text{Zn}]$ ratio in the same sample have been reported separately (Pettini et al. 1997). Recently, Lu et al. (1996) have addressed similar questions from measurements of $[\text{Fe}/\text{H}]$ in 20 DLAs using high-resolution echelle spectra acquired with the Keck telescope. These authors reach conclusions which are in agreement with those presented here regarding the emergence of heavy elements at high redshifts, although the analysis of $[\text{Fe}/\text{H}]$ is complicated by the fact that this ratio, unlike $[\text{Zn}/\text{H}]$, depends on *both* the metallicity and dust content of the interstellar medium.

Before proceeding it is useful to point out that in cases where DLAs from the present sample have been reobserved with HIRES on Keck (Wolfe et al. 1994; Wolfe 1995; Prochaska & Wolfe 1997a), $[\text{Zn}/\text{H}]$ has been found to be in good agreement with the values measured in our survey, which is based on 4-m telescope data (see §2 below). While the exceptional quality of the Keck observations has made possible several new aspects of this work, including the study of the relative abundances of a wide range of elements and the analysis of the kinematics of the absorbing gas, the basic survey of metallicity in DLAs can be carried out satisfactorily with 4-m class telescopes.

The main reason for this is the optically thin nature of the Zn II and Cr II lines in most DLAs proposed by Pettini et al. (1990) and confirmed by subsequent Keck spectra.

2. OBSERVATIONS AND DATA REDUCTION

The new data reported in this paper consist of observations of 10 DLAs in 9 QSOs obtained between March 1994 and February 1996 (an additional candidate DLA from the low dispersion survey by Storrie-Lombardi et al. (1996b)—at $z_{\text{abs}}=3.259$ in the $z_{\text{em}}=4.147$ BAL QSO 1144–073—was shown not to be a damped system by our higher resolution observations of the Lyman α absorption line). In Table 1 we have collected relevant information for the 10 DLAs; the references listed in column (4) are the papers where the damped nature of the absorber was first identified. The absorption redshifts measured from associated metal lines in our blue and red spectra are listed in column (5); with 6 new DLAs at $z_{\text{abs}} > 2.5$, we have tripled the number of absorbers in this redshift regime compared with our earlier sample.

The observations, reduction of the spectra and derivation of Zn and Cr abundances followed the procedures described in Pettini et al. (1994) and the interested reader is referred to that paper for a detailed treatment. Briefly, the observations were carried out mostly with the double-beam cassegrain spectrograph of the William Herschel telescope on La Palma, Canary Islands; additional red spectra were secured with the cassegrain spectrograph of the Anglo-Australian telescope at Siding Spring Observatory, Australia. At $z_{\text{abs}} > 2.5$ the Zn II $\lambda\lambda 2025.483, 2062.005$ and Cr II $\lambda\lambda 2055.596, 2061.575, 2065.501$ multiplets are redshifted longwards of 7175 \AA , where the quantum efficiency of CCDs falls with increasing wavelength. Using EEV and Tektronix CCDs we generally found it necessary to integrate for longer than $\sim 20\,000 \text{ s}$ (column 8 of Table 1) in order to achieve S/N between 9 and 46 (column 9). With a spectral resolution of $0.75\text{--}1.1 \text{ \AA}$ FWHM (column 7), the corresponding 3σ detection limits for the rest frame equivalent widths

of unresolved Zn II and Cr II absorption lines range from $W_0(3\sigma) = 66$ to $14 \text{ m}\text{\AA}$ (column 10). The final “depth” of the survey—that is the lowest metallicity that can be measured—depends on the combination of $W_0(3\sigma)$ and the neutral hydrogen column density $N(\text{H}^0)$. Since the values of $N(\text{H}^0)$ in the new DLAs observed span one order of magnitude (see §3 below), it is the sight-lines with the largest column densities of gas which provide the most stringent limits on metal abundances. Accordingly, we have tended to select DLAs for the present survey primarily on the basis of the value of $N(\text{H}^0)$.

In Figure 1 we have reproduced portions of the QSO spectra encompassing the regions where the Zn II and Cr II lines are expected in the 10 DLAs in Table 1. As can be seen from the figure, the absorption lines sought are detected in approximately half of the cases. Table 2 lists redshifts and rest-frame equivalent widths for the detections; in the other cases the 3σ limits given in column (10) of Table 1 apply.

With the double-beam spectrograph on the WHT we were able to record portions of the blue spectrum of each QSO, centred on the damped Lyman α line, simultaneously with the red arm observations aimed at the Zn II and Cr II lines. The blue detector was either the Image Photon Counting System or a thinned Tektronix CCD; exposure times were the same as those given in column (8) of Table 1. A 600 grooves/mm grating was used to record a 800 \AA wide interval of the spectrum with a resolution of $\sim 1.5 \text{ \AA}$ FWHM. This configuration was chosen in preference to the higher resolving power achievable with a 1200 grooves/mm grating because a good definition of the QSO continuum is a key factor in determining the accuracy with which $N(\text{H}^0)$ can be deduced from the profile of the damping wings of the Lyman α absorption line. Normalised portions of the blue spectra are shown in Figure 2 together with our fits to the damped Lyman α lines. The theoretical damping profiles are centred at the redshifts of the O I $\lambda 1302.1685$ lines which are encompassed by our blue data.

3. ZINC AND CHROMIUM ABUNDANCES

The main results of our survey are collected in Table 3 which includes the 10 DLAs in Table 1 and 7 additional systems for which data have been published since our earlier study (Pettini et al. 1994). Values of the neutral hydrogen column density $N(\text{H}^0)$ are listed in column (3) of Table 4; the typical accuracy of these measurements, including the uncertainty in the placement of the continuum, is $\pm 20\%$. $N(\text{H}^0)$ is likely to account for most of the neutral gas in each DLA given the low molecular fractions which apply to these absorbers at high redshifts (Levshakov et al. 1992; Ge & Bechtold et al. 1997; Ćirković et al. 1997).

Columns (3) and (6) of Table 3 give the column densities of Zn^+ and Cr^+ respectively, deduced from the measured equivalent widths (or upper limits) assuming no line saturation. That this is generally the case is indicated by: (1) the weakness of the absorption lines; (2) the equivalent width ratios of lines within each multiplet which, when measurable, are usually close to the ratios of the corresponding f -values (Bergeson & Lawler 1993); and (3) the resolved absorption profiles recorded with HIRES on Keck for many DLA systems, including some in common with the present survey (Lu et al. 1996; Prochaska & Wolfe 1997a). There are of course exceptions, such as the $z_{\text{abs}} = 2.5842$ system in Q1209+093—see the discussion at §3.12 below. The important point, however, is that it is usually possible with the signal-to-noise ratio and resolution of our data to assess the degree of saturation of the Zn II and Cr II lines.

Column (4) lists the ratios $N(\text{Zn}^+)/N(\text{H}^0)$ derived by dividing the entries in column (3) by those in column (3) of Table 4; comparison with the solar abundance of Zn, $\log (\text{Zn}/\text{H})_{\odot} = -7.35$ (Anders & Grevesse 1989), then leads to *underabundances* of Zn by the factors given in column (5). The corresponding values for Cr ($\log (\text{Cr}/\text{H})_{\odot} = -6.32$) are given in column (8) and column (9) lists the ratio $N(\text{Cr}^+)/N(\text{Zn}^+)$ in cases where it could be determined.

In taking the ratios $N(\text{Zn}^+)/N(\text{H}^0)$ and $N(\text{Cr}^+)/N(\text{H}^0)$ as measures of (Zn/H) and (Cr/H) ,

we implicitly assume that there is little contribution to the observed Zn II and Cr II absorption from ionised gas (which would not produce Lyman α absorption). This is likely to be the case given the large column densities of H I, and indeed there are no indications to the contrary in our data. In particular, we found no significant differences in redshift between the Zn II and Cr II lines, when detected, and O I λ 1302.1685 which arises only in H I regions. Should this assumption be shown to be incorrect, however, the values of [Zn/H] and [Cr/H] deduced here would then be upper limits to the true abundances.

We now comment briefly on each DLA in Table 3.

3.1. Q0000–263; $z_{\text{abs}} = 3.3901$

Our observations of this DLA, the highest redshift absorber in the survey, have been described in Pettini et al. (1995a). While Zn II λ 2025.483 remains undetected, despite the sensitive limit reached in a total exposure time of 58 200 s, we do record weak Cr II absorptions at the 4σ (λ 2055.596) and 3σ (λ 2061.575) significance levels. Cr II λ 2055.596 is expected to be stronger than Zn II λ 2025.483 if the fraction of Cr locked up in dust grains is less than about 50%. With $N(\text{H}^0) = (2.5 \pm 0.5) \times 10^{21} \text{ cm}^{-2}$ (Savaglio, D’Odorico, & Moller 1994), this is one of the highest column density systems in our sample. We conclude that the abundance of Zn is less than 1/80 of the solar value; this estimate is ~ 5 times more sensitive than the previous limit (Savaglio et al. 1994). The abundance of Cr, $[\text{Cr}/\text{H}] \simeq -2.2 \pm 0.1$, is similar to those of other elements measured by Molaro et al. (1996) and Lu et al. (1996), making this DLA one of the most metal-poor in our sample.

3.2. Q0056+014; $z_{\text{abs}} = 2.7771$

This QSO is from the Large Bright Quasar Survey by Chaffee et al. (1991). We deduce $N(\text{H}^0) = (1.3 \pm 0.2) \times 10^{21} \text{ cm}^{-2}$ from fitting the core of the damped Lyman α line, in reasonable agreement with the value $\log N(\text{H I}) = 21.0$ reported by Wolfe et al. (1995).

As can be seen from Figure 1, the Zn II and Cr II absorption lines are broad and shallow in this DLA, spanning $\approx 200 \text{ km s}^{-1}$. The stronger member of the Zn II doublet, $\lambda 2025.483$, falls within the atmospheric A band. Plotting the four absorption lines labelled in Figure 1 on the same velocity scale suggests that most of feature “1” is *not* due to Zn II $\lambda 2025.483$, but rather to poorly corrected telluric absorption. From the equivalent widths of Cr II $\lambda 2055.596$ and $\lambda 2065.501$ (features 2 and 4 in Figure 1), which are consistent with the optically thin ratio of 2:1, we deduce a weighted mean $N(\text{Cr}^+) = (2.8 \pm 0.4) \times 10^{13} \text{ cm}^{-2}$. This column density of Cr^+ produces an equivalent width $W_0 = (82 \pm 12) \text{ m}\text{\AA}$ for Cr II $\lambda 2061.575$; since we measure $W_0 = (117 \pm 16) \text{ m}\text{\AA}$ for feature 3, which is a blend of Cr II $\lambda 2061.575$ and Zn II $\lambda 2062.005$, we conclude that $W_0 = (35 \pm 20) \text{ m}\text{\AA}$ for the latter. This in turn corresponds to $N(\text{Zn}^+) = (3.5 \pm 2) \times 10^{12} \text{ cm}^{-2}$. Thus both Zn and Cr appear to be ≈ 20 times less abundant than in the Sun.

Our red spectrum also shows several Fe II lines from an absorption system at $z_{\text{abs}} = 2.3044$, including: Fe II $\lambda 2344.214$ (visible in Figure 1 at $\lambda_{\text{obs}} = 7748.46\text{\AA}$) with $W_0 = (470 \pm 12) \text{ m}\text{\AA}$; Fe II $\lambda 2367.5905$ with $W_0 = (64 \pm 6) \text{ m}\text{\AA}$; Fe II $\lambda 2374.4612$ with $W_0 = (220 \pm 14) \text{ m}\text{\AA}$; and Fe II $\lambda 2382.765$ with $W_0 = (640 \pm 12) \text{ m}\text{\AA}$.

3.3. Q0201+365; $z_{\text{abs}} = 2.462$

Keck observations of this DLA have been published recently by Prochaska & Wolfe (1996) who deduced relatively high abundances of Zn and Cr, respectively $\sim 1/2$ and $\sim 1/8$ of solar. Evidently, even at redshifts as high as 2.5 some galaxies had already undergone significant chemical evolution and enriched their interstellar media in heavy elements to levels comparable with that of the Milky Way today.

3.4. Q0302–223; $z_{\text{abs}} = 1.0093$

Lanzetta, Wolfe, & Turnshek (1995) proposed this as a candidate DLA system on the basis of low-resolution *IUE* data; a subsequent UV spectrum secured with the Faint Object Spectrograph on the *Hubble Space Telescope* confirmed that $N(\text{H}^0) = (2.15 \pm 0.35) \times 10^{20} \text{ cm}^{-2}$ (Pettini & Bowen 1997). Recent WHT observations of Zn II and Cr II lines by Pettini & Bowen (1997) have shown the abundances to be $1/3$ and $1/8$ of solar respectively. After subtraction of the QSO radial profile from *HST* WFPC2 images of the field, Le Brun et al. (1997) identified two galaxies which may be producing the absorption; at $z = 1.009$ they would have luminosities $L \approx 0.2L^*$ and $\approx L^*$ and distances of 12 and 27 h_{50}^{-1} kpc respectively from the QSO sight-line.

3.5. Q0454+039; $z_{\text{abs}} = 0.8596$

The abundances of Zn and Cr reported by Steidel et al. (1995a) correspond to $[\text{Zn}/\text{H}] = -0.83 \pm 0.08$ and $[\text{Cr}/\text{H}] = -1.01 \pm 0.05$ if the experimentally measured f -values of the Zn II and Cr II multiplets (Bergeson & Lawler 1993) are adopted for consistency with the rest of the present study. Deep images of the QSO field both from the ground (Steidel et al. 1995a) and with *HST*

(Le Brun et al. 1997) suggest that the absorber is a compact galaxy with $L \approx 0.25L^*$ ($q_0 = 0.05$) at a projected distance of $8 h_{50}^{-1}$ kpc from the QSO.

3.6. Q0836+113; $z_{\text{abs}} = 2.4651$

This is the faintest QSO in our survey (Hunstead, Pettini, & Fletcher 1990) and the S/N of the red spectrum remains modest despite the considerable investment in exposure time (Table 1). Combined with the relatively low H I column density of $(3.8 \pm 0.4) \times 10^{20} \text{ cm}^{-2}$, the 3σ upper limits to the Zn II and Cr II lines place limits on the abundances of Zn and Cr which are less stringent than in most other DLAs considered: $[\text{Zn}/\text{H}] \leq -0.8$ and $[\text{Cr}/\text{H}] \leq -1.2$.

The blue spectrum shown in Figure 2 was recorded with the IPCS on the WHT in March 1994. Note that, of all the damped Lyman α lines reproduced in Figure 2, this is the only instance where there appears to be weak emission in the core of the absorption line. The line flux, $(2 \pm 0.7) \times 10^{-17} \text{ erg s}^{-1} \text{ cm}^{-2}$, agrees within the errors with the value of $(2.9 \pm 0.7) \times 10^{-17} \text{ erg s}^{-1} \text{ cm}^{-2}$ reported by Hunstead et al. (1990) from independent data obtained in April 1987 with a different IPCS detector on the AAT. The two sets of observations were obtained with the same slit width (1.2 arcsec) and at the same position angle on the sky (150 degrees).

3.7. Q0841+129; $z_{\text{abs}} = 2.3745, 2.4764$

The spectrum of this bright ($V \simeq 17$), high redshift ($z \simeq 2.5$, estimated from the onset of the Lyman α forest) BL Lac object discovered by C. Hazard (private communication) shows *two* DLAs (see Figure 2), making it a highly suitable target for follow-up high resolution observations.

As can be seen from Figure 1, in the lower redshift system we detect features 2 and 3; the strength of the latter indicates a significant contribution from Zn II $\lambda 2062.005$ to the blend. Following a procedure similar to that described for Q0056+014 at §3.1 above, we deduce $N(\text{Cr}^+) = (9.5 \pm 2) \times 10^{12} \text{ cm}^{-2}$ from the equivalent widths of Cr II $\lambda 2055.596$ and $\lambda 2065.501$. This in turn leads us to estimate that approximately half of the equivalent width of feature 3 is due to Zn II $\lambda 2062.005$ with $W_0 = (24 \pm 9) \text{ m\AA}$. Together with the 3σ upper limit $W_0(2025) \leq 26 \text{ m\AA}$ for the stronger member of the doublet, this then implies $N(\text{Zn}^+) = (1.8 \pm 0.5) \times 10^{12} \text{ cm}^{-2}$.

Thus we find that Zn and Cr at $z_{\text{abs}} = 2.3745$ are underabundant by factors of 23 and 45 respectively, relative to solar values. Similar, or lower, abundances apply to the $z_{\text{abs}} = 2.4764$ DLA, given the lack of detectable Zn II and Cr II lines (see Table 3).

3.8. Q0913+072; $z_{\text{abs}} = 2.6183$

The signal-to-noise ratios of our spectra of this bright QSO are among the highest in the survey—see Table 1 and Figures 1 and 2. The column density of neutral hydrogen is however comparatively low, $N(\text{H}^0) = (2.3 \pm 0.4) \times 10^{20} \text{ cm}^{-2}$. The lack of Zn II and Cr II absorption even at $S/N = 46$ implies underabundances by factors of more than 14 and 32 respectively.

3.9. Q0935+417; $z_{\text{abs}} = 1.3726$

Lanzetta et al. (1995) estimated $N(\text{H}^0) \simeq 2 \times 10^{20} \text{ cm}^{-2}$ for this candidate DLA from low resolution *IUE* data; a subsequent *HST* FOS spectrum confirmed that $N(\text{H}^0) = (2.5 \pm 0.5) \times 10^{20} \text{ cm}^{-2}$ (Lanzetta & Meyer 1996, private communication). With this value of the hydrogen column density, the observations by Meyer, Lanzetta, & Wolfe (1995) imply $[\text{Zn}/\text{H}] = -0.80$ and $[\text{Cr}/\text{H}] = -0.90$.

3.10. Q1104–180; $z_{\text{abs}} = 1.6616$

Smette et al. (1995) identified this DLA in the spectrum of the brighter ($B = 16.7$) component of this gravitationally lensed QSO pair. From AAT observations obtained with an instrumental setup similar to that used in our survey, these authors estimated $N(\text{H}^0) = 6 \times 10^{20} \text{ cm}^{-2}$. They also reported detections of Zn II and Cr II absorption lines with equivalent widths $W_0(2025.483) = (75 \pm 20) \text{ m}\text{\AA}$ and $W_0(2055.596) = (57 \pm 20) \text{ m}\text{\AA}$ respectively. If the lines are unsaturated $[\text{Zn}/\text{H}] = -0.80$ and $[\text{Cr}/\text{H}] = -1.30$.

3.11. Q1151+068; $z_{\text{abs}} = 1.7736$

Even though the damped Lyman α line falls in the crowded near-UV spectrum of this $z_{\text{em}} = 2.762$ QSO (see Figure 2), our estimate $N(\text{H}^0) = (2.0 \pm 0.5) \times 10^{21} \text{ cm}^{-2}$ is in very good agreement with $\log N(\text{H I}) = 21.3$ published by Turnshek et al. (1989). The ratios of equivalent widths within the Zn II and Cr II multiplets strongly suggest that the lines are optically thin; Zn and Cr are both underabundant by a factor ≈ 40 .

Our red spectrum, which covers the region $5500 - 5900 \text{ \AA}$, shows three C IV $\lambda\lambda 1548, 1550$ doublets at $z_{\text{abs}} = 2.5629, 2.7069$ and 2.7551 respectively.

3.12. Q1209+093; $z_{\text{abs}} = 2.5843$

This is another high column density DLA; we measure $N(\text{H}^0) = (2.0 \pm 0.5) \times 10^{21} \text{ cm}^{-2}$ which compares well with $\log N(\text{H I}) = 21.4$ reported by Lu et al. (1993). The Zn II and Cr II

lines are the strongest encountered in the entire survey of 34 DLAs (see Table 2). Fitting the absorption profiles requires $b = 50 \text{ km s}^{-1}$ (as usual, $b = \sqrt{2}\sigma$ where σ is the one-dimensional velocity dispersion along the line of sight), indicating that several velocity components most likely contribute to the absorption. Similarly, Lu et al. found $b = 122 \text{ km s}^{-1}$ from fitting a single curve-of-growth to the strongest UV absorption lines. Some of the components may well be saturated; so we quote our best estimates of $N(\text{Zn}^+)$ and $N(\text{Cr}^+)$ as lower limits. We conclude that Zn is *more* abundant than 1/9 solar and Cr more abundant than 1/27 solar. Higher resolution observations are required to establish how close to these limits the true values are.

3.13. Q1328+307; $z_{\text{abs}} = 0.6922$

We have included here the measurements of Zn and Cr abundances in the spectrum of 3C 286 reported by Meyer & York (1992), after appropriate rescaling with the f -values of Bergeson & Lawler (1993). Although the measurement was discussed in Pettini et al. (1994), this intermediate redshift DLA was not explicitly included in that sample which consisted exclusively of DLAs at $z_{\text{abs}} > 1.7$. CCD images of the QSO field obtained with ground-based telescopes (Steidel et al. 1994) and with *HST* (Le Brun et al. 1997) show a large ($\approx 10 - 30 h_{50}^{-1} \text{ kpc}$), low surface brightness galaxy which has been proposed as the absorber.

3.14. Q1337+113; $z_{\text{abs}} = 2.7957$

Our measured $N(\text{H}^0)$ of $(8 \pm 2) \times 10^{20} \text{ cm}^{-2}$ agrees very well with $\log N(\text{H I}) = 20.9$ reported by Turnshek et al. (1989). When we observed this QSO, in March 1994, we found it to be considerably fainter than the magnitude $V \simeq 18.2$ estimated by Hazard et al. (1986) from POSS plates. Although the S/N achieved is the lowest in the survey (see Table 1 and Figure 1), it is

still sufficient to establish that the abundances of Zn and Cr are less than 1/10 and 1/23 of solar respectively.

3.15. Q1946+769; $z_{\text{abs}} = 2.8443$

This $z_{\text{em}} = 3.051$ QSO, intrinsically one of the most luminous known, is sufficiently bright to have been studied extensively at echelle resolutions and high S/N with 4-m telescopes (Fan & Tytler 1994; Lu et al. 1995; Tripp, Lu, & Savage 1996). However, the hydrogen column density in the $z_{\text{abs}} = 2.8443$ DLA is relatively low, $N(\text{H}^0) = (2 \pm 0.5) \times 10^{20} \text{ cm}^{-2}$ (Lu et al.). Consequently, the upper limits $[\text{Zn}/\text{H}] \leq -0.82$ and $[\text{Cr}/\text{H}] \leq -1.00$ deduced by these authors are rather uninformative given that the true metallicity is ~ 30 times lower ($[\text{Fe}/\text{H}] = -2.44 \pm 0.13$).

3.16. Q2239–386; $z_{\text{abs}} = 3.2810$

This QSO is faint and the absorber is at high redshift; the combination of these two factors resulted in the longest integration time in the survey (see Table 1). Adopting $N(\text{H}^0) = 5.8 \times 10^{20} \text{ cm}^{-2}$ measured by Lu & Wolfe (1994), we deduce Zn and Cr underabundances by factors of more than 11 and 13 respectively.

The Cr measurement is based on the weakest member of the triplet, Cr II $\lambda 2065.501$; $\lambda 2061.575$ is affected by a strong sky emission line and $\lambda 2055.596$, which at $z_{\text{abs}} = 3.2810$ is redshifted to $\lambda_{\text{obs}} = 8802.82 \text{ \AA}$, falls very close to Mn II $\lambda 2606.462$ at $z_{\text{abs}} = 2.3777$, the redshift of a second DLA along this line of sight (Lu & Wolfe 1994). Based on the strengths of the other two members of the Mn II triplet, $\lambda 2576.877$ at $\lambda_{\text{obs}} = 8703.55 \text{ \AA}$ and $\lambda 2594.499$ at $\lambda_{\text{obs}} = 8763.97 \text{ \AA}$, the feature labelled 2 in the last panel of Figure 1 is mostly Mn II $\lambda 2606.462$. The two strong absorption lines also visible in this figure are Fe II $\lambda \lambda 2586.6500, 2600.1729$ at $z_{\text{abs}} = 2.3777$.

4. DISCUSSION

Our total sample, which consists of measurements (or upper limits) of $[\text{Zn}/\text{H}]$ in 34 DLAs over the redshift range $z_{\text{abs}} = 0.6922 - 3.3901$, is constructed by combining data for the 17 DLAs in Table 3 with those for the 15 DLAs in Table 3 of Pettini et al. (1994) and with the further addition of two DLAs in Q0528–250 (Meyer et al. 1989) which were included in the sample considered by Pettini et al. (1994) but not listed in their Table 3. All the points in Figure 3 are based on the f -values of the Zn II doublet by Bergeson & Lawler (1993) and the meteoritic solar abundance of Zn from the compilation by Anders & Grevesse (1989)².

We now consider what implications can be drawn from this extensive survey on the chemical evolution of the neutral content of the universe and on the relationship of damped Lyman α systems to present-day spiral galaxies.

4.1. Chemical Evolution of Damped Lyman α Systems

Figure 3 shows the abundance of Zn as a function of redshift. The enlarged sample confirms the two main conclusions reached by Pettini et al. (1994):

(1) Damped Lyman α systems, *at all redshifts probed*, are generally metal-poor and presumably arise in galaxies at early stages of chemical evolution.

(2) There appears to be a large range in the values of metallicity reached by different galaxies at the same redshift, pointing to a protracted ‘epoch of galaxy formation’ and to the fact that

²This set of atomic parameters and solar abundance introduces a correction of -0.148 to the values of $[\text{Zn}/\text{H}]$ published in Pettini et al. (1994)

chemical enrichment probably proceeded at different rates in different DLA galaxies.

While we find gas with near-solar metallicities at redshifts as high as $z \simeq 2.5$, there are also examples of galaxies with abundances less than 1/10 solar at a time when the disk of the Milky Way differed little from its present-day composition. At redshifts $z \simeq 2 - 2.5$ the full range of metal abundances spans about two orders of magnitude. Although for metallicities $Z_{\text{DLA}} \lesssim 1/50 Z_{\odot}$ the Zn II lines become vanishingly small and only upper limits to the abundance of Zn can be deduced, we do know from echelle spectroscopy of more abundant astrophysical elements that values of $Z_{\text{DLA}} \lesssim 1/100 Z_{\odot}$ are not uncommon at $z_{\text{abs}} = 2 - 3$ (see Figure 1 of Pettini et al. 1995a).

These two results are considered quantitatively in Table 5 where in the last column we list, for various subsets of our sample, the column density-weighted mean abundance of Zn

$$[\langle \text{Zn}/\text{H}_{\text{DLA}} \rangle] = \log \langle (\text{Zn}/\text{H})_{\text{DLA}} \rangle - \log (\text{Zn}/\text{H})_{\odot}, \quad (1)$$

where

$$\langle (\text{Zn}/\text{H})_{\text{DLA}} \rangle = \frac{\sum_{i=1}^n N(\text{Zn}^+)_i}{\sum_{i=1}^n N(\text{H}^0)_i}, \quad (2)$$

and σ' , the standard deviation from the column density weighted mean, defined as

$$(n - 1) \sigma'^2 = \sum_{i=1}^n ([\text{Zn}/\text{H}]_i - [\langle \text{Zn}/\text{H}_{\text{DLA}} \rangle])^2 \quad (3)$$

The summations in equations (2) and (3) are over the n DLA systems considered in each subsample.

Under the working assumption that DLAs account for most of the material available for star formation at high redshift, the quantity $[\langle \text{Zn}/\text{H}_{\text{DLA}} \rangle]$ is a measure of the degree of metal enrichment reached by the universe at a given epoch. This is a general statement which follows from the column density distribution of Lyman α systems (Lanzetta et al. 1995) and which holds

irrespectively of the precise nature of the damped absorbers (disks, spheroids, gas clouds yet to collapse into galaxies, etc.), provided that there are no significant biases in the samples of DLAs from which our observations are drawn (Fall 1996).

The values of $[\langle \text{Zn}/\text{H}_{\text{DLA}} \rangle]$ in Table 5 are strictly upper limits (with the exception of subsample number 1), since the averages include systems for which only upper limits to the abundance of Zn are available. However, we expect the corrections to be small because the systems where the Zn II doublet is below our detection limits are preferentially those with the lowest values of hydrogen column density $N(\text{H}^0)$. Specifically, the fractions of $\sum_{i=1}^n N(\text{H}^0)_i$ contributed by DLAs with undetected Zn II lines are 28% for the full sample, and 16%, 16%, and 37% respectively for subsamples 2, 3 and 4. To show that including the upper limits as detections has only a modest effect on the mean values of metallicity deduced, we have recalculated $[\langle \text{Zn}/\text{H}_{\text{DLA}} \rangle]$ for the full sample twice, substituting 2σ and 1σ limits respectively in place of the 3σ limits used in Table 5 (it could indeed be argued that 3σ limits for the entire ensemble on Zn non-detections is an overly conservative approach). In this case, $[\langle \text{Zn}/\text{H}_{\text{DLA}} \rangle]$ decreases from -1.13 ± 0.38 (the value listed in Table 5) to -1.16 ± 0.40 and -1.20 ± 0.48 respectively. On the other hand, *all* three measurements in subsample 5 ($z_{\text{abs}} = 3.0 - 3.5$) are upper limits and accordingly we quote the value of $[\langle \text{Zn}/\text{H}_{\text{DLA}} \rangle]$ in this redshift interval as an upper limit.

For the full sample of 34 DLAs in the range $z_{\text{abs}} = 0.7 - 3.4$ we find $[\langle \text{Zn}/\text{H}_{\text{DLA}} \rangle] = -1.13 \pm 0.38$. This is the same value as obtained by Pettini et al. (1994) when account is taken of the different f -values and solar abundance scale used in our earlier study. For comparison, $[\text{Zn}/\text{H}]_{\text{gas}} = -0.19$ along unreddened sight-lines in the solar vicinity (Roth & Blades 1995; Sembach et al. 1995—both analyses used the same f -values and solar scale as here). If the interstellar medium (gas+dust) near the Sun has the same composition as the Sun, this would imply that approximately 35% of Zn is in solid form. On the other hand, Pettini et al. (1997) found that for the present sample of DLAs the typical dust-to-metals ratio is approximately half that of the Galactic ISM.

If we assume, therefore, that on average 83% of Zn in DLAs is in the gas phase, we obtain $[\langle \text{Zn}/\text{H}_{\text{DLA}} \rangle] = -1.13 \pm 0.38 + \log(1/0.83) = -1.004 \pm 0.38$, and conclude that the column density weighted abundance of Zn in DLAs is 1/11 of that of the Milky Way ISM today.

One of the motivations of the present work was to determine the redshift evolution of the metallicity of DLAs and thereby trace the increase of heavy elements in the universe from the epoch of galaxy formation to the present time. From Figure 4, where our measures of $[\langle \text{Zn}/\text{H}_{\text{DLA}} \rangle]$ from Table 5 are plotted versus redshift, it can be seen that any such evolution is only mild in the present sample. Between $z = 3$ and 1.5, to which 80% of the sample refers, there appears to be little change from the typical $[\langle \text{Zn}/\text{H}_{\text{DLA}} \rangle] = -1.13$. This is less surprising, however, when one considers that this redshift interval spans a period of only ≈ 3 Gyr from 14.3 to 11.4 Gyr ago ($H_0 = 50 \text{ km s}^{-1} \text{ Mpc}^{-1}$; $q_0 = 0.01$) and that at these epochs evidently there was a large spread in the chemical enrichment of different DLA galaxies.

On the other hand, the upper limit $[\langle \text{Zn}/\text{H}_{\text{DLA}} \rangle] \leq -1.39$ at $z > 3$ is lower than the means in the other redshift bins, providing tentative evidence for a rapid build-up of elements with time at this epoch. This suggestion is strengthened by the data of Lu et al. (1996) who found that $[\text{Fe}/\text{H}] \lesssim -2$ in three additional DLAs at $z > 3$. (The correction to $[\text{Fe}/\text{H}]$ for the fraction of Fe in solid form is likely to be small—probably less than a factor of two—at such low metallicities; Pettini et al. 1997). The lowest metallicities measured in DLAs, $Z_{\text{DLA}} \simeq -2.5$, are comparable to those thought to apply to the ionised intergalactic medium producing the Lyman α forest at redshifts $z = 2 - 3.5$ (Hellsten et al. 1997), although the large ionization corrections involved make estimates of Z_{IGM} considerably more uncertain than Z_{DLA} . It is tempting, therefore, to interpret the rapid increase in metal abundances at $z < 3$ as an indication of the onset of star-formation in galaxies and to speculate that $Z \simeq -2.5$ may be an approximate ‘base’ level of metallicity on which galactic chemical evolution subsequently builds.

The recently realised ability to image high redshift galaxies directly in their ultraviolet stellar

continua has led to the first attempts to sketch the global history of star formation over $\sim 80\%$ of the age of the universe (Madau et al. 1996 and references therein). Determinations of the volume-averaged star formation rate (SFR) from the so-called B and U drop-outs (galaxies with the Lyman limit in the B and U bands respectively) in ground-based surveys (Steidel, Pettini, & Hamilton 1995b) and in the *Hubble Deep Field* (Madau 1996) do indeed suggest an increase in the SFR from $z \simeq 4$ to $z \simeq 2.75$. As discussed by Madau et al., it is possible to convert the integrated UV luminosity density into a metal ejection rate $\dot{\rho}_Z$ per comoving volume at redshift z . Since the massive stars which are the main contributors to the far-UV continuum are also the major producers of heavy elements (at least those released into the ISM by Type II supernovae), the conversion does not depend sensitively on the shape of the IMF in these primordial galaxies. Rather, the principal sources of uncertainty arise from the cosmology assumed and from the amount of dust extinction suffered by the UV continuum.

Bearing in mind these uncertainties, it is of great interest to compare the values of Z_{DLA} deduced here with the metallicities which may be expected on the basis of Madau's metal ejection rate. Integrating $\dot{\rho}_Z$ in Figure 3 of Madau (1996) from $z = 5.5$ to the present time yields a total density of metals $\rho_Z(z = 0) \approx 6.2 \times 10^6 M_\odot \text{ Mpc}^{-3}$. This corresponds to an approximately solar metallicity if the present day density of baryons in galaxies is $\rho_*(z = 0) \approx (2.7 \pm 0.4) \times 10^8 M_\odot \text{ Mpc}^{-3}$, or $\Omega_* \approx 4 \times 10^{-3}$ ($H_0 = 50 \text{ km s}^{-1} \text{ Mpc}^{-1}$; Madau et al. 1996). In a closed box model, assuming that $\Omega_*(z = 0) \approx \Omega_{\text{DLA}}(z = 4)$ (Storrie-Lombardi, McMahon, & Irwin 1996a) we can take

$$\frac{Z(z)}{Z(0)} \simeq \frac{Z(z)}{Z_\odot} = \frac{\int_{5.5}^z \dot{\rho}_Z dz}{\int_{5.5}^0 \dot{\rho}_Z dz} \quad (4)$$

provided the gas consumption into stars from $z = 5.5$ to z is low and $\Omega_{\text{gas}}(z) \gg \Omega_*(z)$. The redshift evolution of Ω_{DLA} (Storrie-Lombardi et al. 1996a) suggests that this may well be the case up to $z \simeq 2$ (as we proposed in Pettini et al. 1994).

The broken line in Figure 4 shows the increase of $Z(z)/Z_{\odot}$ with decreasing redshift calculated from equation (4) and Madau’s (1996) estimates of ρ_Z . Evidently, there is rough agreement between the predicted and observed values of Z_{DLA} . Given the current uncertainties, we consider it premature to read too much into this comparison. For example, Madau’s ρ_Z refers primarily to oxygen and the α -elements which presumably are more abundant than zinc and iron by a factor of 2 – 3 at these low metallicities (Edvardsson et al. 1993; Carney 1996). On the other hand, the broken line in Figure 4 may well underestimate the metal production rate by similar factors if star-forming galaxies at high redshift are reddened by small amounts of dust, corresponding to $E(B - V) \approx 0.1$, as suggested by the observed slopes of the UV continua (Steidel et al. 1996).

Nevertheless, taken at face value, Figure 4 does seem to indicate that in the DLAs we see roughly the same level of metal enrichment as expected from direct observations of star-forming galaxies at these redshifts. More complex galactic chemical evolution models which use as a starting point the gas consumption indicated by the redshift evolution of Ω_{DLA} (Pei & Fall 1995; Fall 1996) also reproduce the degree of metal enrichment of DLAs and the comoving rate of star formation at $z \gtrsim 2$. Thus it appears that, to a first approximation at least, these three independent avenues to exploring the epoch of galaxy formation—the consumption of neutral gas, the metal abundance of the absorbers, and the UV luminosity of high-redshift galaxies—give a broadly consistent picture of the early evolution of galaxies.

4.1.1. Abundances at $z < 1.5$

The situation is less clear at lower redshifts. Only four measurements make up subsample 1 in Table 5, even though this bin spans a larger interval of time than all the other subsets put together— ≈ 5 Gyr from 11.4 to 6.3 Gyr ago (again for $H_0 = 50 \text{ km s}^{-1} \text{ Mpc}^{-1}$; $q_0 = 0.01$). Evidently $[\langle \text{Zn}/\text{H}_{\text{DLA}} \rangle] = -0.98 \pm 0.33$ is below an extrapolation of Madau’s curve in Figure 4.

However, it is difficult to assess how firm this conclusion is, given that 65% of $\sum_{i=1}^n N(\text{H}^0)_i$ for subsample 1 is due to the $z_{\text{abs}} = 0.6922$ absorber in 3C 286 which appears to be a large, low surface brightness galaxy (see §3.13 above). Possibly such galaxies, whose low metallicities at the present time are thought to be the result of low star formation efficiencies (McGaugh 1994; Padoan, Jimenez, & Antonuccio-Delogu 1997), come to dominate the cross-section for DLA absorption at $z \lesssim 1$, if by this epoch most high surface brightness galaxies have already processed a significant fraction of their gas into stars. Furthermore, the build-up of dust which goes hand-in-hand with the production of metals is likely to introduce an increasing bias (with decreasing redshift) against galaxies in advanced stages of chemical evolution, since existing samples of damped Lyman α systems are mostly drawn from magnitude limited optical QSO surveys (Fall & Pei 1993; Pei & Fall 1995).

At $z_{\text{abs}} < 1.5$ imaging of DLA absorbers is within current observational capabilities. Although positive identifications based on spectroscopic redshifts have not yet been achieved, the candidates which have been proposed suggest a very diverse population of galaxies. While in some cases the absorbers could be on evolutionary paths similar to that of the Milky Way, the $z_{\text{abs}} = 1.0093$ DLA in Q0302–223 being a good example (Pettini & Bowen 1997), there are also several instances where galaxies of low luminosity ($L_B \lesssim 0.1L^*$) or of low surface brightness are indicated (Steidel et al. 1994, 1995, 1997; Le Brun et al. 1997).

Thus both effects considered above—a shift of the DLA population away from ‘normal’ L^* galaxies and an increasing dust bias—may contribute to the finding that Z_{DLA} does not increase significantly at $z_{\text{abs}} < 1.5$ in Figures 3 and 4, contrary to simple expectations in a closed-box model of chemical evolution. However, it will not really be possible to proceed further, and quantify the relative importance of these two effects, without a larger sample of DLAs at intermediate redshifts. Identifying such a sample remains an urgent priority.

4.2. Comparison with Stellar Populations of the Milky Way

Damped Lyman α systems are commonly thought of as the high redshift counterparts of present-day galactic disks, although we and others (Pettini et al. 1990; York 1988) have often made the point that high column densities of neutral gas are not the prerogative of disk galaxies alone. The sample of $[\text{Zn}/\text{H}]$ measurements now available is sufficiently large to allow a comparison to be made of the distribution of metallicities in DLAs with those of different stellar populations in the Milky Way. In the solar cylinder, stars in the halo, thick disk, and thin disk have distinct dynamical and abundance properties, although the distributions overlap in either parameter taken separately. It is the *combination* of chemical abundance and kinematic data that studies of Galactic evolution have focussed on; here we attempt to use this information to throw light on the nature of DLA galaxies.

Our measurements of $[\text{Zn}/\text{H}]$ from Figure 3 have been plotted in the top panel of Figure 5 after converting redshift to look-back time in a cosmology compatible with stellar ages. The lower panel in Figure 5 shows the age-metallicity relationship for disk stars determined in the landmark study by Edvardsson et al. (1993). This sample includes stars with the kinematics of both thin and thick disk, defined in terms of the mean velocity perpendicular to the Galactic plane: $\langle |W| \rangle = 19 \text{ km s}^{-1}$ and $\approx 42 \text{ km s}^{-1}$ for thin and thick disk stars respectively (Freeman 1991). In constructing their sample, Edvardsson et al. aimed to include approximately equal numbers of stars in each metallicity bin above $Z = 0.1Z_{\odot}$; consequently, metal-poor stars are relatively over-represented in Figure 5.

Stellar ages are notoriously uncertain, as is the mapping of redshift to look-back time. However, even allowing for an arbitrary sliding of the points in Figure 5 along the x -axes, the metallicity measurements in DLAs evidently do not match the chemical evolution of the Milky Way disk. The *typical* value $Z_{\text{DLA}} = -1.13$ is lower than that of even the most metal-deficient stars in the Edvardsson et al. survey, and at all ages the spread of chemical abundances in the

disk is smaller than that of the DLA sample.

This point is reinforced by Figure 6, where we compare the metallicity distribution of DLAs with those of stars in the thin disk, thick disk and halo populations; in Figure 7 we show the comparison with the metallicity histogram for globular clusters. Values for disk stars are from the work by Wyse & Gilmore (1995). These authors combined spectroscopic determinations of $[\text{Fe}/\text{H}]$ for a sample of F and G stars located 1 – 5 kpc from the plane with data for samples near the Sun, paying particular attention to including only stars with potential main-sequence lifetimes greater than 12 Gyr. That is, their combined sample should be complete, in the sense of not missing disk stars which have by now evolved away from the main sequence, and the resulting metallicity distributions presumably provide an integrated record of the chemical evolution of the disk. The thin disk distribution in Figure 6 includes the low metallicity tail discussed by Wyse & Gilmore (1995); similarly, the thick disk histogram is consistent with the metal-weak tail shown in Figure 22 of Beers & Sommer-Larsen (1995). The halo sample is from the survey of high proper-motion stars in the solar neighbourhood by Laird et al. (1988), while the histogram in Figure 7 is based on the distribution of $[\text{Fe}/\text{H}]$ in 40 globular clusters plotted in Figure 16 of Carney et al. (1996).

The comparison between the metallicity distribution of DLAs and those of stellar populations in the Galaxy is complicated by the fact that about half of the values which make up the bins with $[\text{Zn}/\text{H}]_{\text{DLA}} \leq -0.8$ in Figures 6 and 7 correspond to upper limits of $[\text{Zn}/\text{H}]$ in our survey. Were we to exclude the upper limits from the sample, the resulting distribution would be skewed to higher metallicities. This is also the case if they are included in the sample as detections, as we have done; therefore *the true distribution of Z_{DLA} is both broader and shifted towards lower metallicities (by undetermined amounts) than the histogram reproduced in Figures 6 and 7.*

Bearing this in mind, the middle and bottom panels of Figure 6 show that the metallicity distribution of DLA galaxies is different from those of long-lived stars in the Galactic disk. Although there is some overlap with the thick disk histogram, the bulk of stars in the disk of the

Milky Way apparently formed from gas which was significantly more metal-rich than that giving rise to damped Lyman α systems. The narrow distributions for disk stars in Figure 6 reflect the finding by Edvardsson et al. (1993) that the average metallicity has increased very little over the lifetime of the disk; the scatter at any age in the bottom panel of Figure 5 is nearly as large as the difference in mean metallicity over the entire time span considered. This is also the case for the old open clusters of the Milky Way disk (Friel 1995).

The width of the Z_{DLA} distribution is comparable to those of halo stars and globular clusters, but it peaks at a higher metallicity. This is probably a real effect, rather than being due to the inclusion of upper limits in our sample (as discussed above), since the column density weighted mean metallicity is $[\langle Z_{\text{n}}/H_{\text{DLA}} \rangle] = -1.13$. We consider it unlikely that the offset between the observed and true peaks of the Z_{DLA} distribution is as large as required to bring the histograms in the top panel of Figure 6 and in Figure 7 into agreement. Rather we favour the interpretation that, as a whole, the population of DLA galaxies is genuinely more metal enriched than the stellar components of the Galactic halo.

The comparisons discussed above lead to two possible conclusions concerning the nature of damped Lyman α galaxies. The most straightforward interpretation is that a wide range of galaxy morphological types, at different stages of chemical evolution, make up the the DLA population. Available imaging data at $z \lesssim 1$ are certainly consistent with this view. A more intriguing possibility is that DLA systems at high redshift arise primarily in the spheroidal component of the present-day galaxy population, by analogy with the interpretation of the U drop-out galaxies put forward by Steidel et al. (1995, 1996). In the Milky Way, the halo and inner bulge may well be related, with the halo having lost $\approx 90\%$ of its mass to the bulge (e.g. Wyse, Gilmore, & Franx 1997); in this picture the halo-bulge system is an evolutionary sequence parallel to that of the thick disk-thin disk. One could speculate, then, that the distribution of Z_{DLA} , with its peak at a higher metallicity than halo stars and globular clusters, reflects different stages in the transition

from metal-poor halo to a predominantly metal-rich bulge (Ibata & Gilmore 1995).

4.2.1. *Divergent Clues from the Absorption Line Profiles?*

The message conveyed by Figure 6 contrasts with the interpretation by Wolfe and collaborators of the complex absorption line profiles, often extending over more than 100 km s^{-1} , revealed by high resolution spectroscopy of DLAs (Wolfe 1995; Prochaska & Wolfe 1997b). These authors have argued that in many cases the different components which make up the absorption lines are not distributed at random in velocity; rather, there appears to be a more regular trend of decreasing optical depth with increasing velocity difference from the wavelength where the absorption is strongest. This ‘edge-leading asymmetry’ is the pattern which would be produced by a rotating thick disk, intersected at some distance from the centre, if the average density of gas falls off with distance from the centre and from midplane. Prochaska & Wolfe show that the frequency with which such absorption profiles are encountered is consistent with expectations for randomly oriented disks; this leads them to conclude that most, if not all, DLAs arise in large ($R > 10 \text{ kpc}$) disks with high rotation velocities ($v_{\text{rot}} \gtrsim 200 \text{ km s}^{-1}$). Such structures, if common at $z \gtrsim 2$, are very difficult to explain in currently favoured models of galaxy formation (e.g. Baugh et al. 1997).

The Milky Way is the only galaxy for which we have a record of both chemical abundances and kinematics over its past history. Based on this body of data, the metallicities we measure in the damped Lyman α systems appear incompatible with the rotating disk interpretation put forward by Prochaska & Wolfe. This can be appreciated by considering compilations of metallicities and velocities now available for large samples of stars, such as that published recently by Carney et al. (1996). From their Figures 1 and 3 it can be seen that, of the stars with metal abundances similar to those of DLAs, approximately half have *retrograde* motions; at a metallicity $Z = -1.1$ the mean velocity relative to the disk rotation is $\langle V \rangle \simeq -150 \text{ km s}^{-1}$. This point is best

illustrated by Figure 5 of Carney et al. which shows the metallicity histograms in various intervals of V ; our distribution of Z_{DLA} corresponds to values of V in the range ≈ -100 to ≈ -200 km s $^{-1}$. Evidently, when our Galaxy had an average metallicity of $\lesssim 1/10$ of solar, it did not exhibit the kinematics of a disk rotating at ~ 200 km s $^{-1}$.

Reconciling these contrasting clues to the nature of damped Lyman α galaxies is an important task for the future. Here we put forward three possible ways out of the current impasse:

1. Our Galaxy is atypical, and the physical processes which gave rise to its stellar populations were not shared by most other galaxies at high redshifts. Although this possibility cannot be discounted, it is not a very constructive hypothesis to take refuge in, as it will be difficult to test it observationally—at least in the near future.

2. The absorption profiles are being overinterpreted. A possible concern here is that material whose motion is due not to rotation but to energetic events, such as supernova shocks, may contribute to the ultraviolet absorption lines, since these transitions are sensitive to even relatively small column densities of gas. The ‘edge-leading asymmetry’ interpretation was first proposed by Lanzetta & Bowen (1992) in their analysis of 13 Mg II absorption components spread over 250 km s $^{-1}$ in the $z_{\text{abs}} = 0.39498$ DLA in Q1229–021. However, it is far from clear that this is really a massive disk; from their analysis of *HST* images of the field, Le Brun et al. (1997) propose that the absorber is instead a faint ($L_B < 0.1L^*$) low surface brightness galaxy. Furthermore, strong Mg II absorption spanning ≈ 300 km s $^{-1}$ can also be produced by galaxies which are nearly face-on, such as M61 (Bowen, Blades, & Pettini 1996). All these factors cast some doubts on a detailed correspondence between the profiles of ultraviolet absorption lines and the large-scale kinematics of the intervening galaxies.

3. A third option, and one which we have already proposed, is that DLA galaxies comprise a mix of different morphological types. Thus, it is conceivable that some do exhibit the kinematics of rapidly rotating disks, while others may be spheroids or irregular star-forming galaxies with less

ordered velocity fields. This is a hypothesis which *can* be tested. As more cases become available where both kinematics and chemical abundances are measured in the same DLA, it will be of great interest to examine whether there is any correlation between these two parameters, as found in the stellar populations of the Milky Way.

5. SUMMARY AND SUGGESTIONS FOR FUTURE WORK

We have assembled the largest sample of damped Lyman α systems for which metallicities have been measured free from the complications introduced by dust depletions. The expanded data set reinforces the two main conclusions reached in our earlier study (Pettini et al. 1994): (1) DLAs are generally metal-poor, *at all redshifts sampled*; and (2) there is a large spread in abundances at all epochs. We interpret these findings as evidence for a protracted epoch of galaxy formation, and propose that galaxies of different morphological types and at different stages of chemical evolution make up the DLA population.

The metallicity distribution of DLAs is broader and peaks at lower metallicities than those of either the thin or thick disk of our Galaxy. Thus, the chemical abundance data presented here do not support the interpretation of the absorption line profiles in terms of thick disks with rotation velocities $v_{\text{rot}} \gtrsim 200 \text{ km s}^{-1}$ most recently discussed by Prochaska & Wolfe (1997b). This apparent discrepancy may be resolved by further work on both the kinematics and the abundances. With the near-infrared spectrographs now being built for 8-10 m telescopes it will be possible to detect the familiar optical emission lines from star-forming regions in the absorbing galaxies. The widths of these features are likely to be more representative of the global kinematics than the ultraviolet absorption lines which can be so easily affected by local phenomena such as interstellar shocks. On the abundance front, the ratios of chemical elements manufactured in different nucleosynthetic processes have been used to good effect in unravelling the history of star formation in our Galaxy;

the same techniques are now beginning to be applied to high redshift DLAs (Pettini et al. 1995b; Lu et al. 1996).

The column density weighted mean metallicity of DLAs at $z \gtrsim 2$ is in agreement with expectations based on the metal ejection rate deduced by Madau (1996) from the integrated ultraviolet luminosity of star forming galaxies at these redshifts. Our data, when combined with the [Fe/H] measurements by Lu et al. (1996), appear to reflect the rapid increase in the comoving star-formation rate between $z \approx 4$ and ≈ 2 indicated by the relative numbers of B and U drop-outs in the *Hubble Deep Field*. While these comparisons are of necessity still very approximate, the implication seems to be that observations of DLAs provide a reasonably accurate census of metal enrichment at these epochs. It is encouraging that three independent methods which have been applied to the quest for the epoch of galaxy formation—the global star formation rate deduced from the ultraviolet luminosity of high-redshift galaxies, the rate of consumption of neutral gas implied by the redshift evolution of Ω_{DLA} , and the metallicity of DLAs—apparently give a broadly consistent picture of the universe at $z \gtrsim 2$.

This is not the case at $z \lesssim 1.5$, where Z_{DLA} apparently does not rise as expected from simple models of cosmic chemical evolution. There are a number of plausible explanations for this, including the effects of dust, as discussed extensively by Fall and collaborators, and an increasing contribution of low surface brightness galaxies to the cross-section for DLA absorption. The major obstacle to progress in this area is still the paucity of DLAs with measured element abundances at intermediate redshifts. And yet it is essential to follow the evolution of the DLA population to the present time in order to be confident of our interpretation of the high redshift data. New DLAs at $z \lesssim 1$ are still being identified and the sample is slowly growing. With STIS on the *HST* measurements of [Zn/H] can be extended to redshifts lower than the limit $z_{\text{abs}} \simeq 0.65$ of ground-based observations. In the next few years the 2dF and Sloan sky surveys (Taylor 1995; Gunn & Weinberg 1995) are expected to increase the number of known DLAs by one order of

magnitude. With 8-10 m telescopes it will then be possible to repeat surveys such as this one towards substantially fainter, and potentially more reddened, QSOs. Such programmes should lead to a better assessment of the significance of dust bias in current DLA samples. Finally, with large telescopes we will soon be able to measure element abundances from the optical emission lines of galaxies at redshifts $z \approx 0.1 - 0.5$. Such data will complement in a very important way the information provided by galaxies selected from their absorption cross-section.

We are grateful to the UK and Australian Time Assignment committees for generous allocations of telescope time on the WHT and the AAT, and to the technical staff at both Observatories for excellent support with the observations. The WHT Service Observations scheme helped bring this demanding observing programme to completion. We should like to express our sincere thanks to: C. Hazard and P. Hewett for supplying us with positions and finding charts of QSOs with candidate damped Lyman α systems; J. Lewis for assistance with the reduction of some of the spectra; J. Laird and R. Wyse for providing the stellar data used in Figures 6 and 7; C. Jenkins and K. Lipman for help with some statistical aspects of the analysis; M. Fall, G. Gilmore, P. Madau, and S. Ryan for illuminating discussions on several issues relating to stellar populations and galactic chemical evolution; and C. Steidel, J. Prochaska, and D. York for useful comments on an earlier version of the paper. R.W.H. acknowledges financial assistance from the Australian Research Council.

REFERENCES

- Anders, E., & Grevesse, N. 1989, *Geochim. Cosmochim. Acta*, 53, 197
- Baugh, C.M., Cole, S., Frenk, C.S., & Lacey, C.G. 1997, *ApJ*, submitted (astro-ph/9703111)
- Beers, T.C., & Sommer-Larsen, J. 1995, *ApJS*, 96, 175
- Bergeson, S.D., & Lawler, J.E. 1993, *ApJ*, 408, 382
- Bowen, D.V., Blades, J.C., & Pettini, M. 1996, *ApJ*, 472, L77
- Carney, B.W. 1996, *PASP*, 108, 900
- Carney, B.W., Laird, J.B., Latham, D.W., & Aguilar, L.A. 1996, *AJ*, 112, 668
- Chaffee, F.H., Foltz, C.B., Hewett, P.C., Francis, P.A., Weymann, R.J., Morris, S.L., Anderson, S.F., & MacAlpine, G.M. 1991, *AJ*, 102, 461
- Ćirković, M.M., Lanzetta, K.M., Baldwin, J., Williger, G., Carswell, R.F., Potekhin, A.Y., & Varshalovich, D.A. 1997, *ApJ*, submitted
- Edvardsson, B., Andersen, J., Gustafsson, B., Lambert, D.L., Nissen, P.E., & Tomkin, J. 1993, *A&A*, 275, 101
- Fall, S.M. 1996, in *HST and the High Redshift Universe*, ed. N. Tanvir, A. Aragon-Salamanca, & J.V. Wall (Singapore: World Scientific), in press.
- Fall, S.M., & Pei, Y.C. 1993, *ApJ*, 402, 479
- Fan, X.M., & Tytler, D. 1994, *ApJS*, 94, 17
- Freeman, K.C. 1991, in *Dynamics of Disc Galaxies*, ed. B. Sundelius (Göteborg University, Göteborg), 15
- Friel, E.D. 1995, *ARAA*, 33, 381
- Ge, J., & Bechtold, J. 1997, *ApJ*, in press (astro-ph/9701041)

- Gunn, J.E., & Weinberg, D.H. 1995, in *Wide Field Spectroscopy and the Distant Universe*, ed. S.J. Maddox & A. Aragon-Salamanca, (Singapore: World Scientific), 3
- Hazard, C. 1994, private communication
- Hazard, C., McMahon, R.G., & Morton, D.C. 1987, *MNRAS*, 229, 371
- Hazard, C., Morton, D.C., McMahon, R.G., Sargent, W.L.W., & Terlevich, R. 1986, *MNRAS*, 223, 87
- Hellsten, U., Davé, R., Hernquist, L., Weinberg, D.H., & Katz, N. 1997, *ApJ*, in press (astro-ph/9701043)
- Hunstead, R.W., Pettini, M., & Fletcher, A.B. 1990, *ApJ*, 365, 23
- Ibata, R.A., & Gilmore, G. 1995, *MNRAS*, 275, 605
- Laird, J.B., Rupen, M.P., Carney, B.W., & Latham, D.W. 1988, *AJ*, 96, 1908
- Lanzetta, K.M., & Bowen, D.V. 1992, *ApJ*, 391, 48
- Lanzetta, K.M., Wolfe, A.M., & Turnshek, D.A. 1995, *ApJ*, 440, 435
- Le Brun, V., Bergeron, J., Boisse, P., & Deharveng, J.M. 1997, *A&A*, in press
- Levshakov, S.A., Chaffee, F.H., Foltz, C.B., & Black, J.H. 1992, *A&A*, 262, 385
- Lu, L., Sargent, W.L.W., Barlow, T.A., Churchill, C.W., & Vogt, S.S. 1996, *ApJS*, 107, 475
- Lu, L., Savage, B.D., Tripp, T.M., & Meyer, D.M. 1995, *ApJ*, 447, 597
- Lu, L., & Wolfe, A.M. 1994, *AJ*, 108, 44
- Lu, L., Wolfe, A.M., Turnshek, D.A., & Lanzetta, K.M. 1993, *ApJS*, 84, 1
- Madau, P., 1996, in *Star Formation Near and Far*, Proc. 7th Annual Astrophysics Conference in Maryland, ed. S.S. Holt & G.L. Mundy (AIP: New York), in press (astro-ph/9612157)
- Madau, P., Ferguson, H.C., Dickinson, M., Giavalisco, M., Steidel, C.C., & Fruchter, A. 1996, *MNRAS*, 283, 1388

- McGaugh, S.S. 1994, *ApJ*, 426, 135
- Meyer, D.M., Lanzetta, K.M., & Wolfe, A.M. 1995, *ApJ*, 451, L13
- Meyer, D.M., Welty, D.E., & York, D.G. 1989, *ApJ*, 343, L37
- Meyer, D.M., & York, D.G. 1992, *ApJ*, 399, L121
- Molaro, P., D’Odorico, S., Fontana, A., Savaglio, S., & Vladilo, G. 1996, *A&A*, 308, 1
- Padoan, P., Jimenez, R., & Antonuccio-Delogu, V. 1997, *ApJ*, in press
- Pei, Y.C., & Fall, S.M. 1995, *ApJ*, 454, 69
- Pettini, M., Boksenberg, A., & Hunstead, R.W. 1990, *ApJ*, 348, 48
- Pettini, M., & Bowen, D.V. 1997, *A&A*, submitted
- Pettini, M., King, D.L., Smith, L.J., & Hunstead, R.W. 1995a, in *QSO Absorption Lines*, ed. G. Meylan (Berlin: Springer-Verlag), 71
- Pettini, M., King, D.L., Smith, L.J., & Hunstead, R.W. 1997, *ApJ*, in press (April 1, 1997 issue)
- Pettini, M., Lipman, K., & Hunstead, R.W. 1995b, *ApJ*, 451, 100
- Pettini, M., Smith, L.J., Hunstead, R.W., & King, D.L. 1994, *ApJ*, 426, 79
- Prochaska, J.X., & Wolfe, A.M. 1996, *ApJ*, 470, 403
- Prochaska, J.X., & Wolfe, A.M. 1997a, *ApJ*, 474, 140
- Prochaska, J.X., & Wolfe, A.M. 1997b, in preparation
- Roth, K.C., & Blades, J.C. 1995, *ApJ*, 445, L95
- Sargent, W.L.W., Boksenberg, A., & Steidel, C.C. 1988, *ApJS*, 68, 539
- Savaglio, S., D’Odorico, S., & Moller, P. 1994, *A&A*, 281, 331
- Sembach, K.R., Steidel, C.C., Macke, R.J., & Meyer, D.M. 1995, *ApJ*, 445, L27
- Smette, A., Robertson, J.G., Shaver, P.A., Reimers, D., Wisotzki, L., & Kohler, T. 1995, *A&A Supp*, 113, 199

- Smith, H.E., Cohen, R.D., & Bradley S.E. 1986, ApJ, 310, 583
- Smith, L.J., Pettini, M., King, D.L., & Hunstead, R.W. 1996, in From Stars to Galaxies—the Impact of Stellar Physics on Galaxy Evolution, ed. C. Leitherer, U. Fritze-von Alvensleben & J. Huchra, Astr. Soc. Pacific Conf. Ser., 98, 559
- Steidel, C.C., Bowen, D.V., Blades, J.C., & Dickinson, M. 1995a, ApJ, 440, L45
- Steidel, C.C., Dickinson, M., Meyer, D.M., Adelberger, K.L., & Sembach, K.R. 1997, ApJ, in press
- Steidel, C.C., Giavalisco, M., Pettini, M., Dickinson, M., & Adelberger, K.L. 1996, ApJ, 462, L17
- Steidel, C.C., Pettini, M., & Hamilton, D. 1995b, AJ, 110, 2519
- Steidel, C.C., Pettini, M., Dickinson, M., & Persson, S.E. 1994, AJ, 108, 2046
- Storrie-Lombardi, L.J., McMahon, R.G., & Irwin, M.J. 1996a, MNRAS, 283, L79
- Storrie-Lombardi, L.J., McMahon, R.G., Irwin, M.J., & Hazard, C. 1996b, ApJ, 468, 121
- Taylor, K. 1995, in Wide Field Spectroscopy and the Distant Universe, ed. S.J. Maddox & A. Aragon-Salamanca, (Singapore: World Scientific), 15
- Tripp, T.M., Lu, L., & Savage, B.D. 1996, ApJS, 102, 239
- Turnshek, D.A., Wolfe, A.M., Lanzetta, K.M., Briggs, F.H., Cohen, R.D., Foltz, C.B., Smith, H.E., & Wilkes, B.J. 1989, ApJ, 344, 567
- Wolfe, A.M. 1995, in QSO Absorption Lines, ed. G. Meylan (Berlin: Springer-Verlag), p.13
- Wolfe, A.M., Fan, X.-M., Tytler, D., Vogt, S.S., Keane, M.J., & Lanzetta, K.M. 1994, ApJ, 435, L101
- Wolfe, A.M., Lanzetta, K.M., Foltz, C.B., & Chaffee, F.H. 1995, ApJ, 454, 698
- Wyse, R.F.G., & Gilmore, G. 1995, AJ, 110, 2771
- Wyse, R.F.G., Gilmore, G., & Franx, M. 1997, ARAA, 35, in press (astro-ph/9701223)

York, D.G. 1988, in QSO Absorption Lines: Probing the Universe, ed. J.C. Blades, D.A. Turnshek,
& C.A. Norman (Cambridge: Cambridge Univ. Press), 227

TABLE 1
DAMPED Ly α SYSTEMS OBSERVED

QSO	V (mag)	z_{em}	Ref.	z_{abs}	Telescope	Resolution (\AA)	Integration Time (s)	S/N	$W_0(3\sigma)^a$ (m \AA)
(1)	(2)	(3)	(4)	(5)	(6)	(7)	(8)	(9)	(10)
0000–263	18	4.111	1	3.3901	AAT	1.1	58200	30	25
0056+014	18.9	3.154	2	2.7771	WHT	1.0	21000	28	28
0836+113	19.4	2.696	3	2.4651	WHT	0.77	34000	14	47
0841+129	17	2.5:	4	2.3745	WHT	0.76	20000	30	23
0841+129	17	2.5:	4	2.4764	WHT	0.76	20000	30	22
0913+072	17.1	2.785	5	2.6183	WHT	0.75	19800	46	14
1151+068	18.8	2.762	6	1.7736	WHT	0.81	14400	44	20
1209+093	18.5	3.297	7	2.5843	WHT	0.82	18000	29	24
1337+113	18.2	2.919	3	2.7957	WHT	0.75	18000	9	66
2239–386	18	3.511	8	3.2810	AAT	1.1	65875	18	43

^a 3σ detection limit for the rest frame equivalent width of an unresolved absorption line.

REFERENCES — (1) Savaglio, D’Odorico, & Moller 1994; (2) Wolfe et al. 1995; (3) Smith, Cohen, & Bradley 1986; (4) Hazard 1994; (5) Sargent, Boksenberg & Steidel 1988; (6) Turnshek et al. 1989; (7) Hazard, McMahon, & Morton 1987; (8) Lu & Wolfe 1994.

TABLE 2
REDSHIFTS AND EQUIVALENT WIDTHS OF Zn II AND Cr II LINES

QSO	Line 1 Zn II λ 2025.483		Line 2 Cr II λ 2055.596		Line 3 Cr II λ 2061.575+ Zn II λ 2062.005	Line 4 Cr II λ 2065.501	
	z_{abs}	W_0 (mÅ)	z_{abs}	W_0 (mÅ)	W_0 (mÅ)	z_{abs}	W_0 (mÅ)
(1)	(2)	(3)	(4)	(5)	(6)	(7)	(8)
0000–263	...	≤ 25	3.3901	31 ± 8	22 ± 7	...	≤ 25
0056+014	... ¹	... ¹	2.7766:	116 ± 17	117 ± 16	2.7769:	49 ± 12
0841+129	...	≤ 26	2.3746	37 ± 7	52 ± 7	...	≤ 23
1151+068	1.7737	49 ± 9	1.7736	78 ± 8	75 ± 8	1.7736	34 ± 6
1209+093	2.5842	190 ± 10	2.5846	185 ± 15	195 ± 15	2.5842	120 ± 15

Notes. — Absorption redshifts are vacuum heliocentric. Equivalent widths are rest-frame values with $\pm 1\sigma$ errors. No redshifts are listed for Line 3 as two absorption lines contribute to the feature.

¹ Blended with atmospheric A band

TABLE 3

Zn AND Cr ABUNDANCES IN THE DAMPED $\text{Ly}\alpha$ SYSTEMS

QSO	z_{abs}	$N(\text{Zn}^+)$ (10^{12} cm^{-2})	$N(\text{Zn}^+)/N(\text{H}^0)$ (10^{-9})	Zn Underabun. Factor	$N(\text{Cr}^+)$ (10^{12} cm^{-2})	$N(\text{Cr}^+)/N(\text{H}^0)$ (10^{-9})	Cr Underabun. Factor	$N(\text{Cr}^+)/N(\text{Zn}^+)$
(1)	(2)	(3)	(4)	(5)	(6)	(7)	(8)	(9)
0000–263	3.3901	≤ 1.4	≤ 0.56	≥ 80	8 ± 1.5	3.1 ± 0.9	155^{+60}_{-35}	≥ 5.5
0056+014	2.7771	3.5 ± 2	2.7 ± 1.6	$17^{+23}_{-6.5}$	28 ± 4	22 ± 5	22^{+6}_{-4}	8 ± 5
0201+365 ^a	2.462	5.9 ± 0.6	24.5 ± 3	1.85 ± 0.2	14.5 ± 1	60 ± 7	8.0 ± 0.9	2.5 ± 0.3
0302–223 ^b	1.0093	3.0 ± 0.6	14 ± 4	$3.2^{+1.3}_{-0.7}$	13 ± 2.5	60 ± 15	$8.0^{+2.6}_{-1.6}$	4.3 ± 1.2
0454+039 ^c	0.8596	3.8 ± 0.7	6.7 ± 1.3	$6.7^{+1.6}_{-1.1}$	27 ± 3	47 ± 5	$10^{+1.5}_{-1}$	7 ± 1.5
0836+113	2.4651	≤ 2.6	≤ 7	≥ 6.5	≤ 12	≤ 32	≥ 15	...
0841+129	2.3745	1.8 ± 0.5	2.0 ± 0.7	23^{+12}_{-6}	9.5 ± 2	10.5 ± 3	45^{+19}_{-10}	5.5 ± 2.5
0841+129	2.4764	≤ 1.2	≤ 2.1	≥ 22	≤ 5.6	≤ 9.3	≥ 51	...
0913+072	2.6183	≤ 0.8	≤ 3.3	≥ 14	≤ 3.4	≤ 15	≥ 32	...
0935+417 ^d	1.3726	1.8 ± 0.4	7 ± 2	$6.5^{+2.5}_{-1.5}$	15 ± 4	60 ± 20	8^{+4}_{-2}	8.5 ± 3
1104–180 ^e	1.6616	4.2 ± 1.1	7 ± 2	$6.5^{+2}_{-1.5}$	15 ± 5	25 ± 9	19^{+11}_{-5}	3.5 ± 1.5
1151+068	1.7736	2.5 ± 0.5	1.25 ± 0.4	36^{+17}_{-9}	22 ± 2	11 ± 3	43^{+60}_{-34}	9 ± 2
1209+093	2.5843	≥ 10	≥ 5	≤ 9	≥ 35	≥ 17.5	≤ 27	...
1328+307 ^f	0.6922	5.3	2.8	16	20	10.5	46	3.8
1337+113	2.7957	≤ 3.7	≤ 4.6	≥ 10	≤ 17	≤ 21	≥ 23	...
1946+769 ^g	2.8443	≤ 1.4	≤ 6.8	≥ 6.7	≤ 9.6	≤ 48	≥ 10	...
2239–386	3.2810	≤ 2.4	≤ 4.2	≥ 11	≤ 22	≤ 38	≥ 13	...

NOTES —

- a* Prochaska & Wolfe 1996
- b* Pettini & Bowen 1997
- c* Steidel et al. 1995
- d* Meyer, Lanzetta, & Wolfe 1995
- e* Smette et al. 1995
- f* Meyer & York 1992
- g* Lu et al. 1995

TABLE 4
H I COLUMN DENSITIES IN THE DAMPED Ly α SYSTEMS

QSO	z_{abs}	$N(\text{H}^0)$ (10^{20} cm^{-2})	FWHM(Ly α) (\AA)
(1)	(2)	(3)	(4)
0000–263	3.3901	25 ± 5^a	...
0056+014	2.7771	13 ± 2	18.0
0201+365 ^b	2.462	2.4 ± 0.2	...
0302–223 ^c	1.0093	2.15 ± 0.35	7.6
0454+039 ^d	0.8596	5.7 ± 0.3	...
0836+113	2.4651	3.8 ± 0.4	10.6
0841+129	2.3745	9 ± 2	15.2
0841+129	2.4764	6 ± 1.5	12.5
0913+072	2.6183	2.3 ± 0.4	8.1
0935+417 ^e	1.3726	2.5 ± 0.5^f	...
1104–180 ^g	1.6616	6	...
1151+068	1.7736	20 ± 5	22.0
1209+093	2.5843	20 ± 5	22.2
1328+307 ^h	0.6922	19	...
1337+113	2.7957	8 ± 2	14.0
1946+769 ⁱ	2.8443	2 ± 0.5	...
2239–386	3.2810	5.8^j	...

NOTES —

^a Savaglio, D’Odorico, & Moller 1994

^b Prochaska & Wolfe 1996

^c Pettini & Bowen 1997

^d Steidel et al. 1995

^e Meyer, Lanzetta, & Wolfe 1995

^f Lanzetta & Meyer 1996, private communication

^g Smette et al. 1995

^h Meyer & York 1992

ⁱ Lu et al. 1995

^j Lu & Wolfe 1994

Table 5. COLUMN DENSITY WEIGHTED METALLICITIES

	Redshift Range	Lookback Time (Gyr) ^a	DLAs	Detections	Upper Limits	$[\langle \text{Zn}/\text{H}_{\text{DLA}} \rangle]$
Full Sample	0.6922 – 3.3901	7.8 – 14.7	34	19	15	-1.13 ± 0.38
Subsample 1	0.50 – 1.49	6.3 – 11.4	4	4	0	-0.98 ± 0.33
Subsample 2	1.50 – 1.99	11.4 – 12.7	8	6	2	-0.96 ± 0.44
Subsample 3	2.00 – 2.49	12.7 – 13.6	12	6	6	-1.23 ± 0.38
Subsample 4	2.50 – 2.99	13.6 – 14.3	7	3	4	-1.11 ± 0.27
Subsample 5	3.00 – 3.49	14.3 – 14.8	3	0	3	≤ -1.39

^a $H_0 = 50 \text{ km s}^{-1} \text{ Mpc}^{-1}$; $q_0 = 0.01$

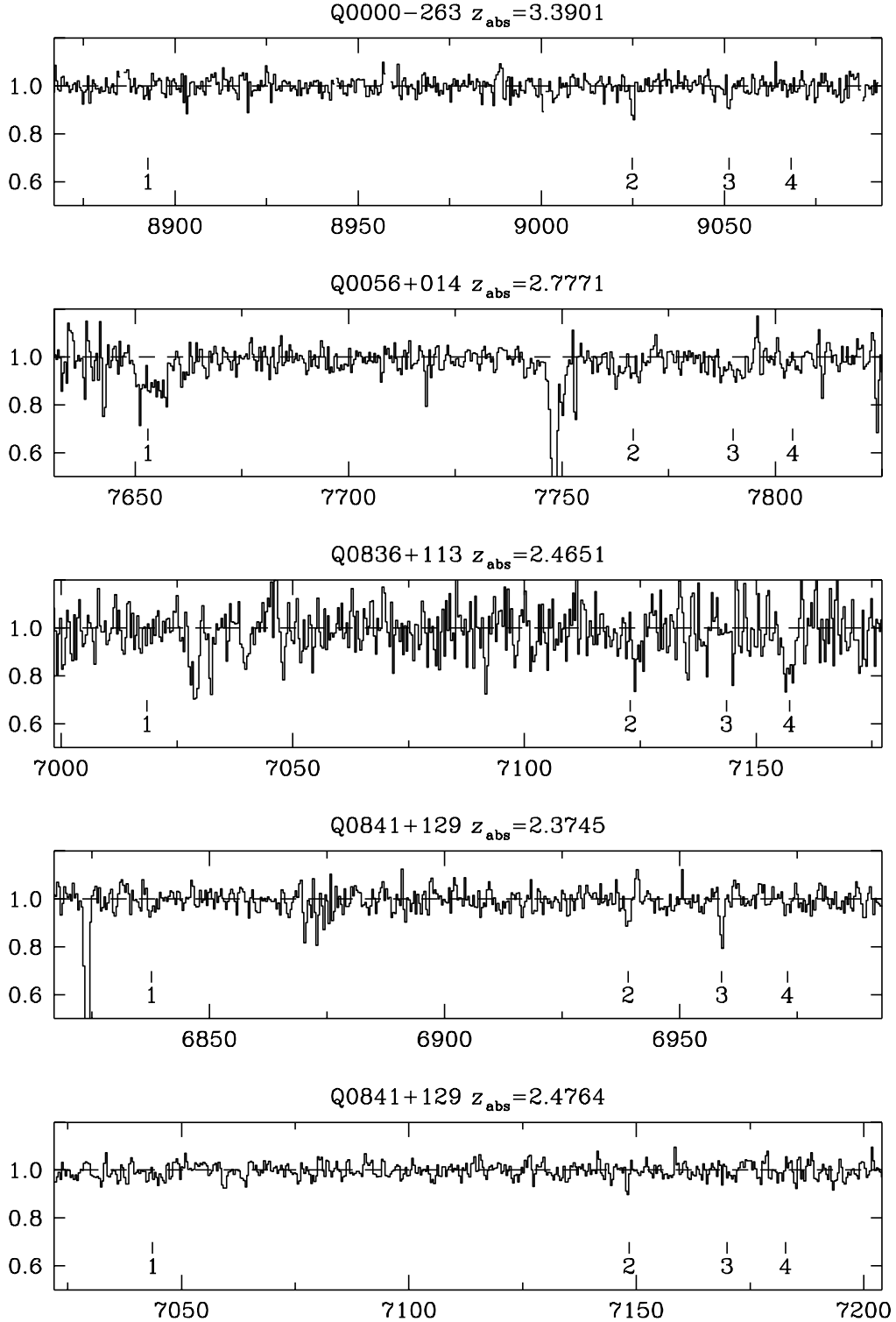
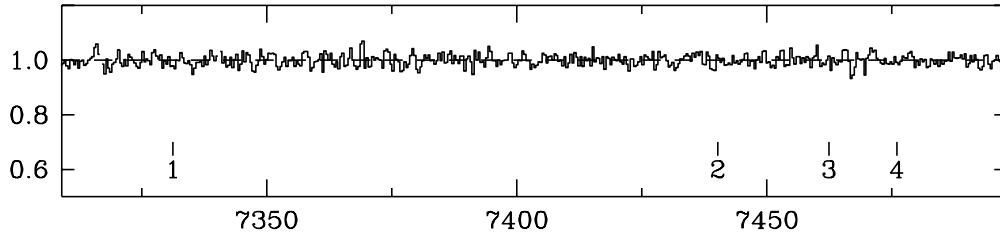
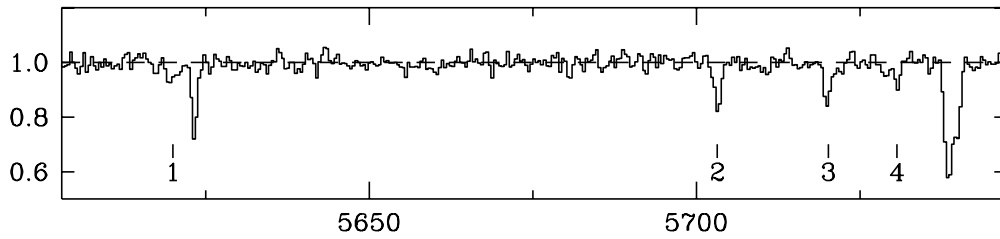


Fig. 1a.— Portions of the QSO spectra observed in our survey of Zn II and Cr II lines in damped Lyman α systems. The x -axis is wavelength in Å; the y -axis is residual intensity. The vertical tick marks indicate the expected positions of the absorption lines, whether they have been detected or not. Line 1: Zn II $\lambda 2025.483$; line 2: Cr II $\lambda 2055.596$; line 3: Cr II $\lambda 2061.575$ + Zn II $\lambda 2062.005$

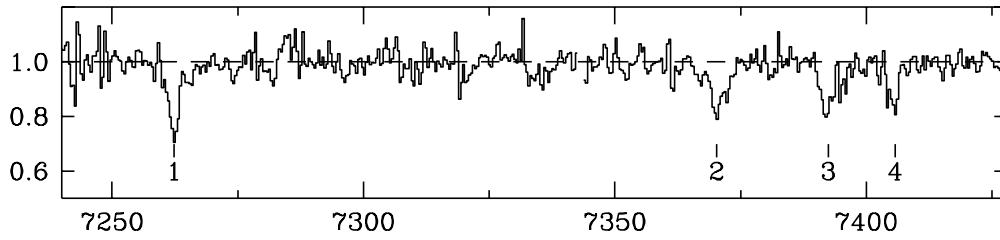
Q0913+072 $z_{\text{abs}}=2.6183$



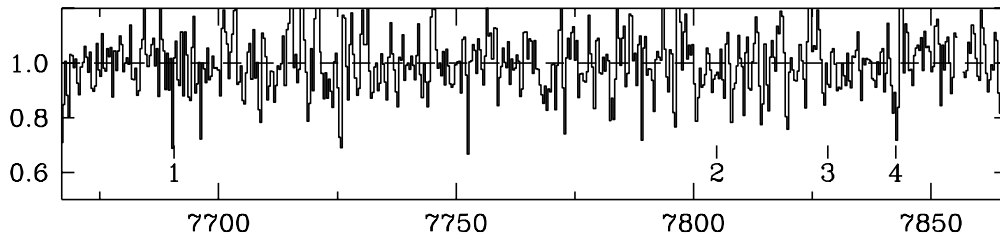
Q1151+068 $z_{\text{abs}}=1.7736$



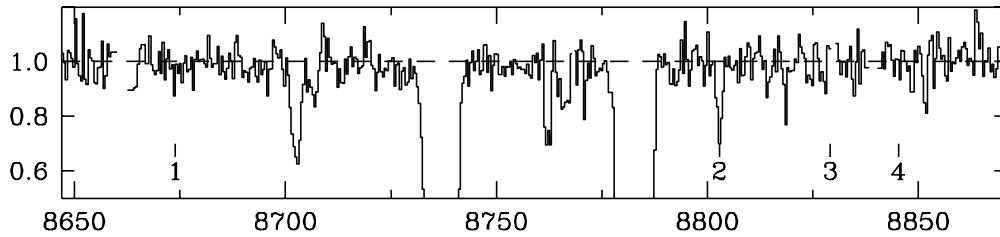
Q1209+093 $z_{\text{abs}}=2.5843$



Q1337+113 $z_{\text{abs}}=2.7957$



Q2239-386 $z_{\text{abs}}=3.2810$



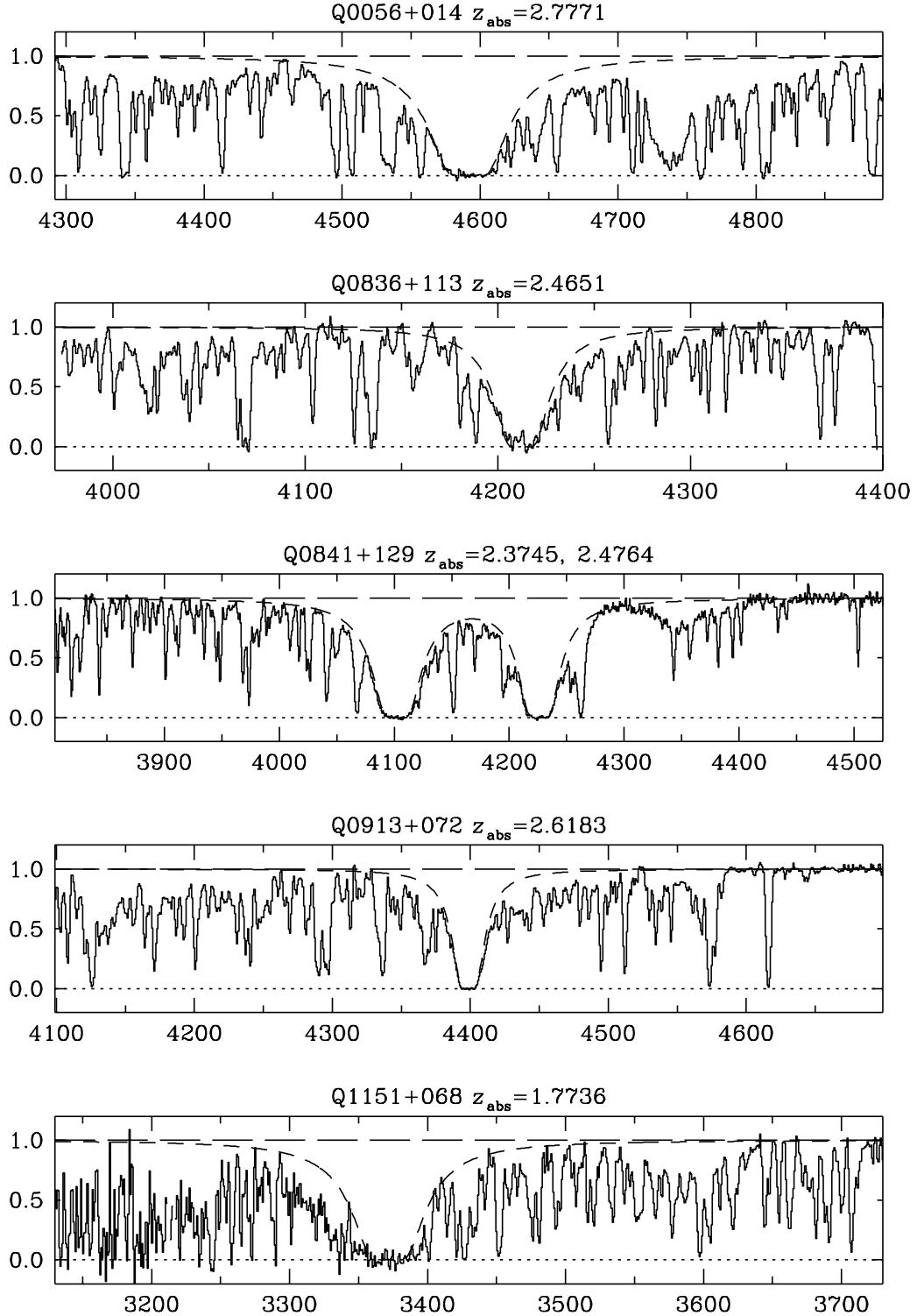


Fig. 2a.— Normalised portions of the blue spectra of QSOs in our survey centred on the damped Lyman α absorption line. The x -axis is wavelength in Å; the y -axis is residual intensity. In each panel the short-dash line shows the theoretical damping profile corresponding to the value of neutral

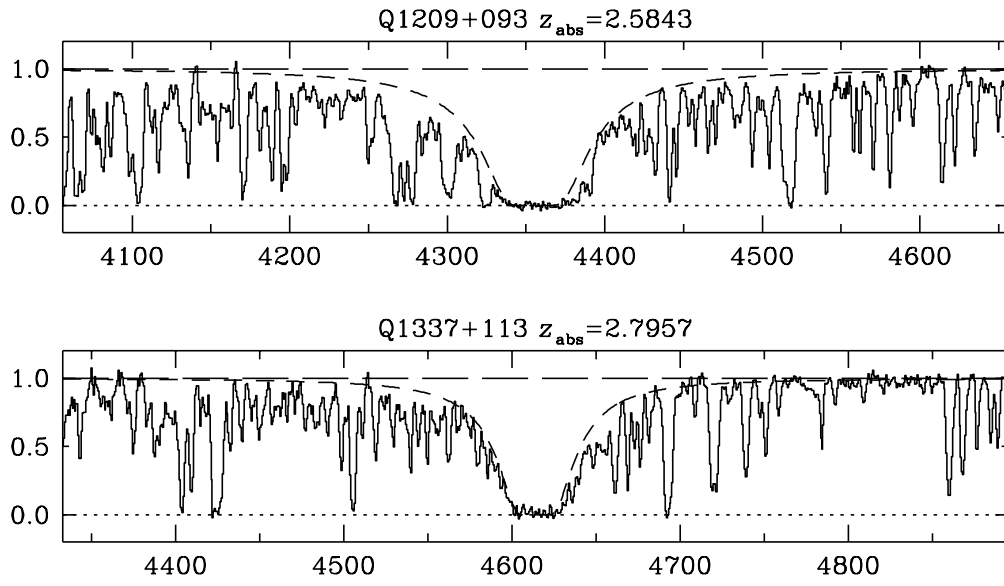


Fig. 2b .— (continued)

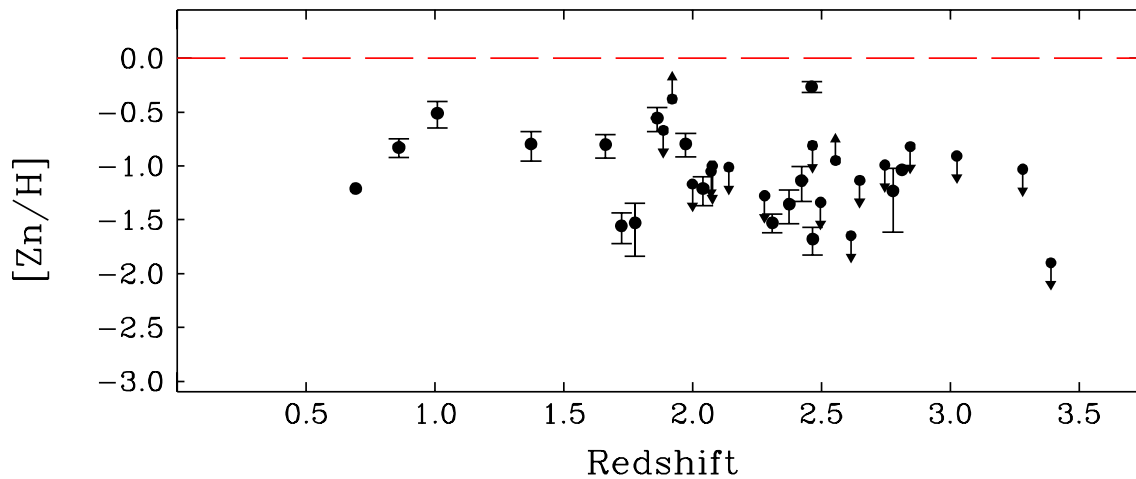


Fig. 3.— The abundance of Zn for the 34 damped Lyman α systems in the present survey plotted against redshift. Abundances are measured on a log scale relative to the solar value shown by the broken line at $[Zn/H] = 0.0$. Upper limits, corresponding to non-detection of the Zn II lines, are indicated by downward-pointing arrows. For two damped systems, indicated by dots with upward-pointing arrows, we derive *lower* limits to the abundances, because the absorption lines may be saturated.

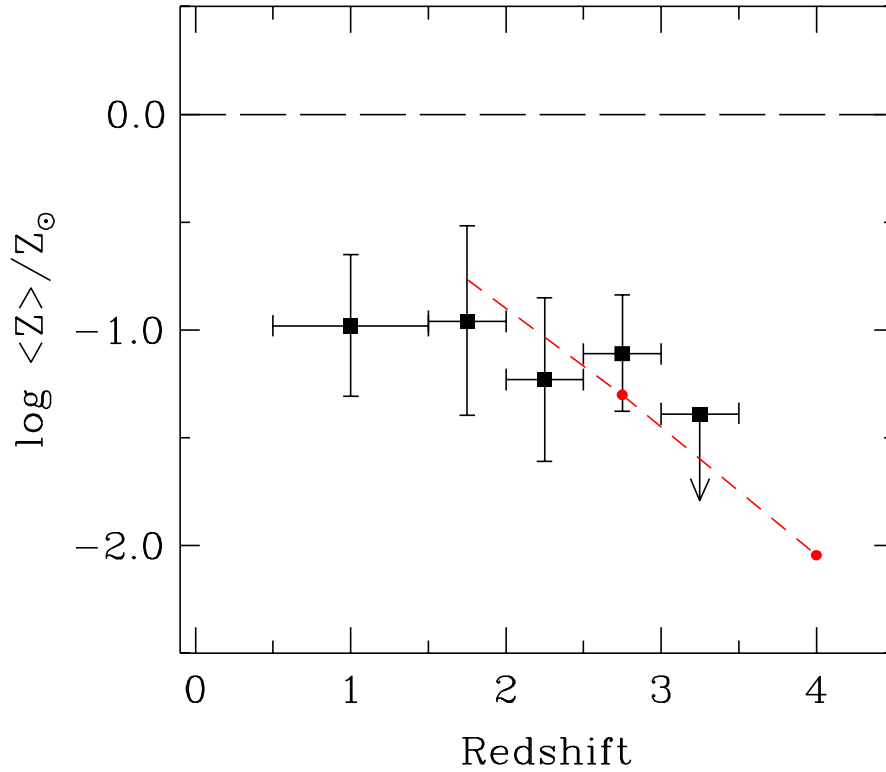


Fig. 4.— Cosmic chemical evolution as deduced from the metallicity of damped Lyman α systems (filled squares) and from the metal ejection rate, ρ_Z , of high redshift galaxies in the *Hubble Deep Field* (dots). The filled squares are the values of $[\langle Z_{\text{n}}/H_{\text{DLA}} \rangle]$ from the present survey; the broken line shows the predictions of a simple integration of the redshift evolution of ρ_Z from Madau (1996) for a $H_0 = 50 \text{ km s}^{-1} \text{ Mpc}^{-1}$ and $q_0 = 0.5$ cosmology. For $q_0 = 0.01$ the broken line would shift to lower values of $\log \langle Z \rangle / Z_{\odot}$ by a factor of ~ 2 .

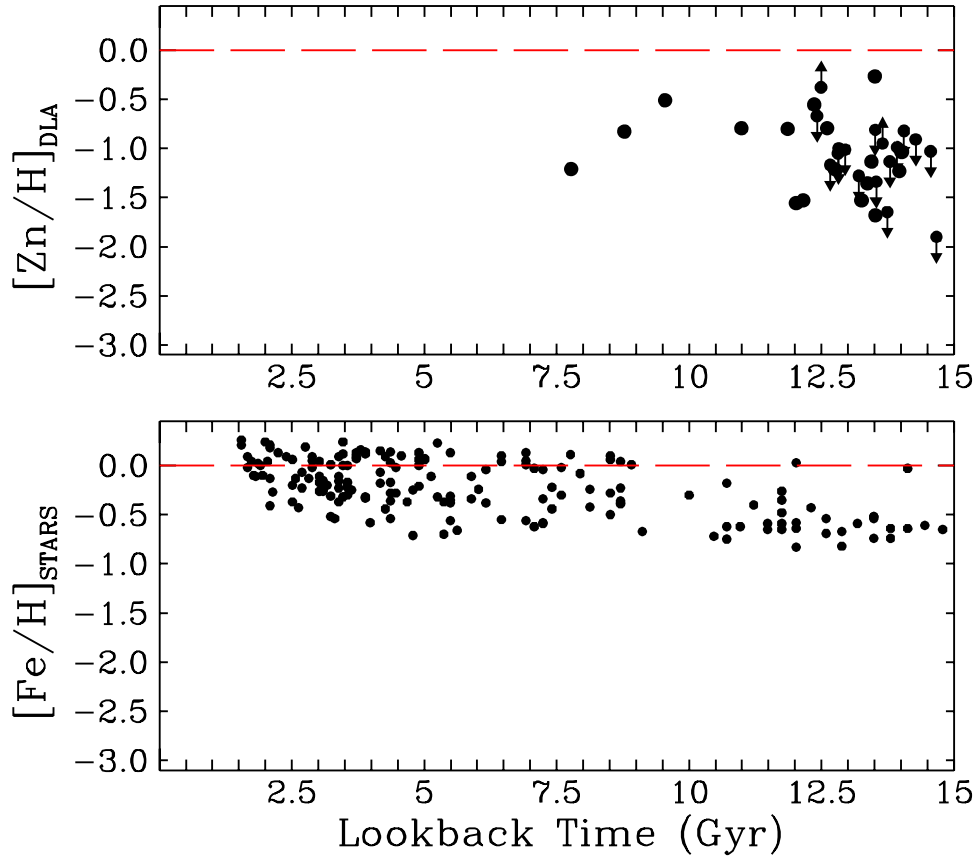


Fig. 5.— *Top Panel:* Available measurements of metallicity in damped Lyman α systems plotted as a function of lookback time for $H_0 = 50 \text{ km s}^{-1} \text{ Mpc}$ and $q_0 = 0.01$. *Bottom Panel:* Metallicities of 182 F and G dwarf stars in the Galactic disk with measured iron abundances and ages from the large-scale study by Edvardsson et al. (1993).

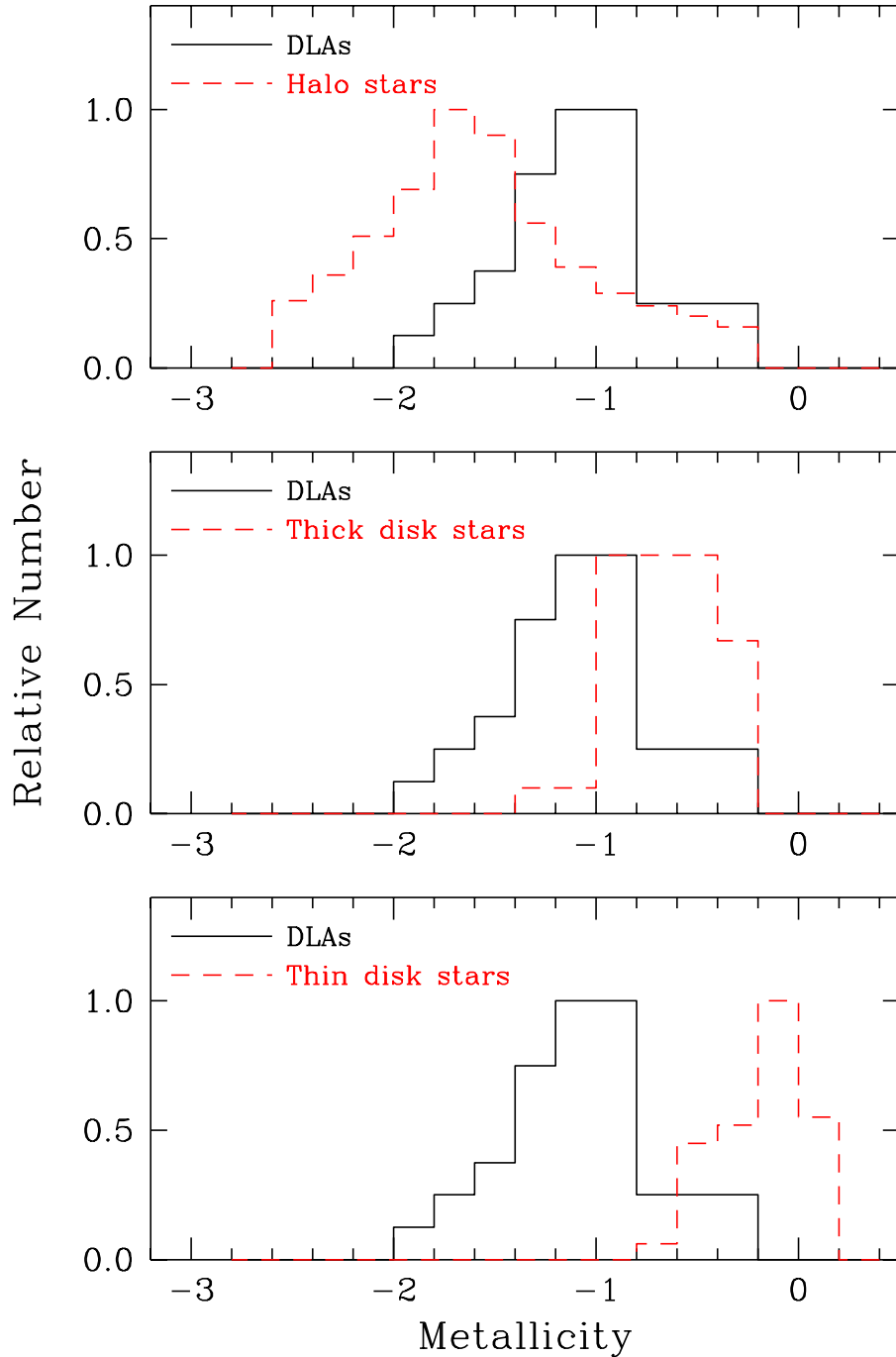


Fig. 6.— Metallicity distributions, normalised to unity, of damped Lyman α systems and of stars belonging to the disk and halo populations in the Milky Way. See text for references to the sources of stellar data. Upper limits to $[\text{Zn}/\text{H}]_{\text{DLA}}$ have been included as measurements in the histogram.

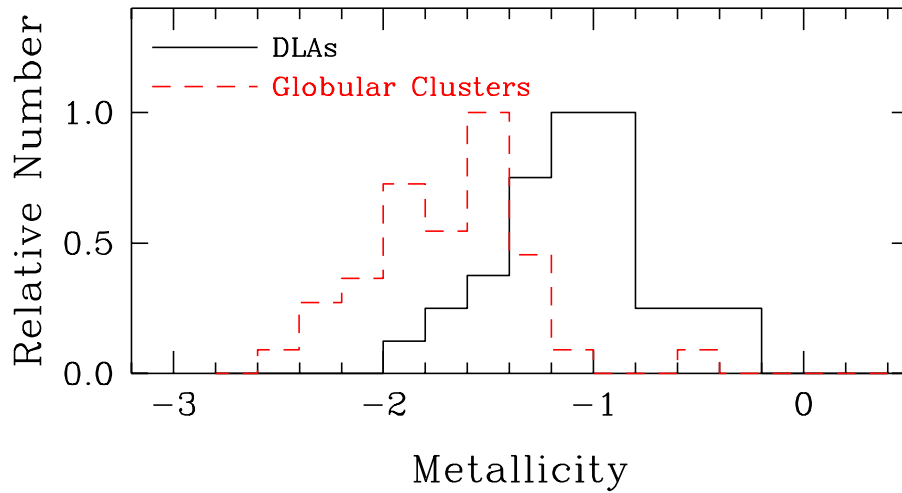


Fig. 7.— Metallicity distributions, normalised to unity, of damped Lyman α systems and of 40 globular clusters in the sample of Carney et al. (1996). Upper limits to $[\text{Zn}/\text{H}]_{\text{DLA}}$ have been included as measurements in the histogram.